A new and trivial CP symmetry for extended A_4 flavor

C. C. Nishi*

Centro de Matemática, Computação e Cognição,

Universidade Federal do ABC - UFABC, 09.210-170, Santo André, SP, Brasil

The combination of ν_μ-ν_τ exchange together with CP conjugation in the neutrino sector (known as $\mathsf{CP}^{\mu\tau}$ symmetry or $\mu\tau$-reflection) is known to predict the viable pattern: $\theta_{23} = 45°$, maximal Dirac CP phase and trivial Majorana phases. We implement such a CP symmetry as a new CP symmetry in theories with A_4 flavor. The implementation in a complete renormalizable model leads to a new form for the neutrino mass matrix that leads to further predictions: normal hierarchical spectrum with lightest mass and $m_{\beta\beta}$ ($0\nu2\beta$) of only few meV, and either ν_1 or ν_2 has opposite CP parity. An approximate $L_\mu - L_\tau$ symmetry arises naturally and controls the flavor structure of the model. The light neutrino masses are generated by the extended seesaw mechanism with 6 right-handed neutrinos (RHNs). The requirement of negligible one-loop corrections to light neutrino masses, validity of the extended seesaw approximation and not too long-lived BSM states to comply with BBN essentially restricts the parameters of the model to a small region: three relatively light right-handed neutrinos at the GeV scale, heavier neutrinos at the electroweak scale and Yukawa couplings smaller than the electron Yukawa. Such a small Yukawa couplings render these RHNs unobservable in terrestrial experiments.

I. INTRODUCTION

The discovery of nonzero $\theta_{13} \sim 8.5°$ in 2012 [1] prompted the neutrino physics community to one of its next experimental goals: measure or discard CP violation in the leptonic sector [2]. As one more parameter in the standard three neutrino paradigm joined the list of known quantities, we are only left with three unknowns in case neutrinos are Majorana: neutrino mass ordering, absolute neutrino mass scale and CP violation in the leptonic sector. The last unknown has three sources: one Dirac CP phase analogous to the CKM phase for quarks and two Majorana phases.

From a theory viewpoint, many symmetries were sought over the years in order to predict the CP violating phases of the leptonic sector. The simplest of them that leads to CP violation and viable mixing angles is known as $\mu\tau$-reflection or $\mathsf{CP}^{\mu\tau}$ which consists on ν_μ-ν_τ flavor exchange together

*Electronic address: celso.nishi@ufabc.edu.br

with CP conjugation [3]. Often, such a CP symmetry is considered in conjunction with nonabelian discrete symmetries [4–7]. In fact, many studies were devoted to the definition of CP symmetry in that context [5–7]. However, differently from many simple flavor symmetries that predicted vanishing θ_{13}, the $\mathsf{CP}^{\mu\tau}$ symmetry allows nonzero θ_{13} but predicts all the presently unknown CP phases: the Dirac CP phase $\delta_{\mathsf{CP}} = \pm 90^\circ$ is maximal while the Majorana phases are trivial [3, 8]. Moreover, θ_{23} is also predicted to be maximal, the neutrinoless double beta decay effective mass is restricted to narrower bands and, in simple implementations, leptogenesis is only allowed to occur in the intermediate range of $T \sim M_1 \sim 10^9 - 10^{12}\,\mathrm{GeV}$ where flavor effects are important [8]. From current global fits [9, 10], we know in fact there is a slight preference for negative δ_{CP} and $\theta_{23} = 45^\circ$ is still allowed.

Two directions were recently pursued to generalize the idea of $\mathsf{CP}^{\mu\tau}$ symmetry. Firstly, we have shown in Ref. [8] that a minimal setting that allowed distinct symmetries in the charged lepton and neutrino sectors consisted of only one abelian symmetry (the combination of lepton flavors $\mathsf{L}_\mu - \mathsf{L}_\tau$ or subgroup) and CP symmetry ($\mathsf{CP}^{\mu\tau}$). This setting was shown to be free from the vev alignment problem that plagues many flavor symmetry models for leptons. In contrast, in Ref. [11], it was shown that maximal θ_{23} and δ_{CP} (the prediction for Majorana phases is lost) could follow from much more general assumptions without the imposition of CP symmetry. The necessary conditions involve the symmetry of the charged lepton sector (G_l) to be represented by *real* matrices in the flavor space and, in the same basis, M_ν needs to be diagonalizable by a *real* matrix. The crucial aspect is the former, which presumably follows from a *real* flavor symmetry conserved in the charged lepton sector. The neutrino sector can not be invariant by the same residual symmetry and hence must have a large breaking in the form of misaligned vevs.

Here we try to embed a subgroup of $\mathsf{L}_\mu - \mathsf{L}_\tau$ into a discrete nonabelian flavor group G_F in order to increase predictivety but, at the same time, retain the successful features of Ref. [8]. We choose the A_4 group which is an extensively studied flavor group (see [12] and references therein). In fact, the first $\mathsf{CP}^{\mu\tau}$ symmetric neutrino mass matrix was obtained with this group [13]. More recent studies involving A_4 and CP can be seen in Refs. [14, 15].

We anticipate that the light neutrino mass matrix in our model will have the form

$$M_\nu = \begin{pmatrix} a_1+a_2+a_3 & k(a_1+\omega a_2+\omega^2 a_3) & k(a_1+\omega^2 a_2+\omega a_3) \\ k(a_1+\omega a_2+\omega^2 a_3) & k^2(a_1+\omega^2 a_2+\omega a_3) & k^2(a_1+a_2+a_3) \\ k(a_1+\omega^2 a_2+\omega a_3) & k^2(a_1+a_2+a_3) & k^2(a_1+\omega a_2+\omega^2 a_3) \end{pmatrix}, \tag{1}$$

where a_i, k are real parameters and $k > 0$ can be chosen; $\omega \equiv e^{i2\pi/3}$ as usual. This mass matrix

is $\mathsf{CP}^{\mu\tau}$ symmetric [3] but has 4 real parameters to describe 5 observables: $\theta_{12}, \theta_{13}, m_1, m_2, m_3$. Hence, we will have one prediction.

The paper is organized as follows: In Sec. II we describe the new CP symmetry that can be implemented for theories with A_4 symmetry. Section III shows that the mass matrix (1) can fit the present oscillation parameters and additionally give predictions for the absolute neutrino mass and CP parities. A complete renormalizable model is shown in Sec. IV where the light neutrino masses are generated by the extended seesaw (ESS) mechanism [17] with relatively light right-handed neutrinos in its spectrum. The approximate symmetry $\mathtt{L}_\mu - \mathtt{L}_\tau$ is presented in Sec. V and shown to constrain the flavor structure of the model. Section VI analyzes the constraints on the model coming from (i) the radiative stability of the tree-level result, (ii) validity of the ESS approximation to fit the light neutrino masses and (iii) sufficiently short-lived BSM states that not spoil Big Bang nucleosinthesis. More phenomenological constraints on the presence of relatively light right-handed neutrinos is analyzed in Sec. VII. The conclusions are shown in Sec. VIII and the appendices contain auxiliary material.

II. ANOTHER GCP FOR A_4

The group $A_4 = (\mathbb{Z}_2 \times \mathbb{Z}_2) \rtimes \mathbb{Z}_3$ have one three dimensional irreducible representation (irrep) $\mathbf{3}$ and three one-dimensional irreps $\mathbf{1'}, \mathbf{1''}, \mathbf{1}$, where the latter is the trivial invariant (singlet). The faithful $\mathbf{3}$ can be generated by

$$a = \mathrm{diag}(1, -1, -1), \quad b = \begin{pmatrix} 0 & 1 & 0 \\ 0 & 0 & 1 \\ 1 & 0 & 0 \end{pmatrix}, \tag{2}$$

where a generates one of the $\mathbb{Z}_2$ subgroups and b generates the $\mathbb{Z}_3$ subgroup. Only b acts non-trivially on the singlets $\mathbf{1'}, \mathbf{1''}$ as

$$\mathbf{1'} \xrightarrow{b} \omega \mathbf{1'}, \quad \mathbf{1''} \xrightarrow{b} \omega^2 \mathbf{1''}, \tag{3}$$

where $\omega = e^{i2\pi/3}$.

For generic settings where generic irreps of A_4 (e.g. a $\mathbf{3}$ and one *charged* $\mathbf{1'}$) are considered in a model, there is only one possible CP symmetry that can be imposed on the model [6, 7]. As first considered in Ref. [4], CP acts on the representations of (2) and (3) as

$$\mathsf{CP}_1: \quad \mathbf{3} \to X\mathbf{3}^*, \quad \mathbf{1} \to \mathbf{1}^*, \quad \mathbf{1'} \to \mathbf{1'}^*, \quad \mathbf{1''} \to \mathbf{1''}^*, \tag{4}$$

where X can be chosen as (23) exchange:

$$X = \begin{pmatrix} 1 & 0 & 0 \\ 0 & 0 & 1 \\ 0 & 1 & 0 \end{pmatrix} . \tag{5}$$

The complex conjugation denotes the CP transformation operation on the fields which should be adjoined with the appropriate Lorentz factors for e.g. spin 1/2 fermions. We denote the whole flavor group considering CP_1 as $A_4 \rtimes \mathbb{Z}_2^{\mathsf{CP}}$ and it gives rise to a group isomorphic to S_4, denoted as $\tilde{S}_4$ in [4]. Obviously any composition of CP_1 with an element of A_4 is also a GCP symmetry, so any of the 12 GCP symmetries can be chosen as a residual symmetry [15].

In nongeneric settings where only a specific set of irreps is considered, it is clear that there is one more inequivalent option. If only $\mathbf{3}$ is considered, we can use the *usual* CP transformation [1]:

$$\mathsf{CP}_2 : \mathbf{3} \to \mathbf{3}^* . \tag{6}$$

Given that the representation (2) is real, the whole group including CP_2 will be denoted as $A_4 \times \mathbb{Z}_2^{\mathsf{CP}}$ where $\mathbb{Z}_2^{\mathsf{CP}}$ is generated by CP_2, which commutes with A_4 ($\mathbf{3}$ is real).

Now the question is: What is the transformation law for the other irreps (if any is consistent)? We can deduce them by noting that the transformation (6) acts on the representation (2) *trivially*, i.e.,

$$\mathsf{CP}_2 : \quad a \to a, \quad b \to b , \tag{7}$$

if we apply on any $\mathbf{3}$, in this order, CP_2, the transformation a or b and then CP_2^{-1}. In contrast, for CP_1, the same set of operations induces

$$\mathsf{CP}_1 : \quad a \to X a^* X^{-1} = a, \quad b \to X b^* X^{-1} = b^2. \tag{8}$$

Here we are identifying a, b with its three dimensional irrep $D_{\mathbf{3}}(a), D_{\mathbf{3}}(b)$ in (2). Given that (8) and (7) lead to different rules (map different conjugacy classes), they can not be equivalent. These mapping rules in the group are called automorphisms and only (8) and (7) are nonequivalent for A_4. So these are the only possibilities for defining GCP in the presence of A_4 symmetry [6].

We can now deduce that one transformation law for the singlets $\mathbf{1}'$ that is compatible with (6) and (7) is the *trivial* transformation

$$\mathsf{CP}_2 : \quad \mathbf{1}' \to \mathbf{1}' . \tag{9}$$

[1] It is important to note that the GCP (4), with symmetric X, can be also cast in the form (6) by basis change, after which the representation (2) changes and is no longer real.

However, this transformation law can be only used if the complex field $\psi_1 \sim \mathbf{1}'$ is neutral under any other group, including the Lorentz group, i.e., it must be a scalar [2]. Moreover, if ψ_1 carries other complex quantum numbers (it excludes $\mathbb{Z}_2$) other than A_4, say a charge q of $U(1)$, then (9) is not compatible with the fact that CP should reverse the charge q. Therefore, in this case another field $\psi_2 \sim \mathbf{1}''$ with the same charge q (or any other quantum number) needs to be introduced to define the transformation

$$\mathsf{CP}_2: \quad \psi_1 \to \psi_2^*\,, \tag{10}$$

so that both sides transform as ω by b but the field of charge q is mapped to a field of charge $-q$. This is also the transformation law for fermions. To summarize, the irreps $\mathbf{1}'$ and $\mathbf{1}''$ are *exchanged* by CP_2,

$$\mathsf{CP}_2: \quad \mathbf{1}' \to \mathbf{1}''^*, \tag{11}$$

unless $\mathbf{1}''^*$ can be identified with $\mathbf{1}'$. Therefore, for charged fields (such as the SM fields or any chiral fermion) the irreps $\mathbf{1}', \mathbf{1}''$ need to be introduced in *pairs*.

The symmetry CP_2 (associated to the trivial automorphism) can be straightforwardly extended for other groups with structure $H \rtimes \mathbb{Z}_3$ such as the $\Delta(3 \cdot N^2) = (\mathbb{Z}_N \times \mathbb{Z}_N) \rtimes \mathbb{Z}_3$ family [e.g. $\Delta(27)$ [16]] or some of its subgroups such as T_7 or T_{13}. The only difference is that the triplet representations are now complex and CP symmetry acts as usual.

We stress that the CP_2 symmetry for A_4 has not been considered for flavor model building before. This possibility is raised in the general context of discrete nonabelian symmetries in [6] but no model application was discussed. For A_4, this possibility is commented in [15] but it is not pursued. Ref. [7] discards this kind of CP symmetry dubbing it as CP-like symmetries but, as we will see for the simple case of A_4, no theoretical consideration prevents its use. As an added bonus, we will see that the transformation property (9) allows us to avoid the vev alignment problem [8].

III. MASS MATRIX

We first analyze our mass matrix (1) in the flavor basis to show that we can correctly fit the oscillation parameters. This is a new form for the neutrino mass matrix that has not been considered so far.

[2] One could also use (9) as charge conjugation for a *pair* of Majorana fermion fields where b acts by 120° rotation in the plane.

The $\mathsf{CP}^{\mu\tau}$ symmetry of (1) implies that $\theta_{23} = \pi/4$ and $\delta_{\mathsf{CP}} = \pm\pi/2$ are automatic [3] and the diagonalization

$$U^{\mathsf{T}} M_\nu U = \mathrm{diag}(m_i')\,, \tag{12}$$

can be performed by a matrix $U = U_0$ of the form

$$U_0 = \begin{pmatrix} u_1 & u_2 & u_3 \\ w_1 & w_2 & w_3 \\ w_1^* & w_2^* & w_3^* \end{pmatrix}\,, \tag{13}$$

with u_i conventionally real and positive. The Majorana phases are trivial and possible CP parities appear along with the eigenvalues $m_i' = \pm m_i$, $m_i \geq 0$. We denote the different cases of CP parities by the sign of (m_i') as

$$(+\,+\,+), (-\,+\,+), (+\,-\,+), (+\,+\,-)\,. \tag{14}$$

In addition to being $\mathsf{CP}^{\mu\tau}$ symmetric, the mass matrix in (1) obeys

$$\begin{aligned} M_\nu\big|_{a_2\leftrightarrow a_3} &= M_\nu^*\,, \\ M_\nu\big|_{a_1\to a_2\to a_3} &= \mathrm{diag}(1,\omega^2,\omega) M_\nu\, \mathrm{diag}(1,\omega^2,\omega)\,. \end{aligned} \tag{15}$$

Thus cyclic permutation of a_i leaves all observables of M_ν invariant while transposition $(a_2 \leftrightarrow a_3)$ flips the Dirac CP phase: $\delta_{\mathsf{CP}} \to -\delta_{\mathsf{CP}}$. Hence, permutations of solutions for a_i are solutions as well.

A. Obtaining the masses

To extract the light neutrino masses, it is more convenient to change to a real basis:

$$M_\nu' = U_{23}^{\mathsf{T}} M_\nu U_{23} = \begin{pmatrix} a_1+a_2+a_3 & \frac{k}{\sqrt{2}}(2a_1-a_2-a_3) & \sqrt{\frac{3}{2}}k(a_3-a_2) \\ \frac{k}{\sqrt{2}}(2a_1-a_2-a_3) & \frac{1}{2}k^2(4a_1+a_2+a_3) & \frac{1}{2}\sqrt{3}k^2(a_2-a_3) \\ \sqrt{\frac{3}{2}}k(a_3-a_2) & \frac{1}{2}\sqrt{3}k^2(a_2-a_3) & \frac{3}{2}k^2(a_2+a_3) \end{pmatrix}\,, \tag{16}$$

where

$$U_{23} \equiv \begin{pmatrix} 1 & 0 & 0 \\ 0 & \frac{1}{\sqrt{2}} & \frac{i}{\sqrt{2}} \\ 0 & \frac{1}{\sqrt{2}} & -\frac{i}{\sqrt{2}} \end{pmatrix}\,. \tag{17}$$

Now M_ν' is real symmetric and can be diagonalized by a real orthogonal matrix.

The eigenvalues of M'_ν will correspond to the light neutrino masses $m'_i = \pm m_i$ with its CP parities. They are solutions of the characteristic equation

$$\lambda^3 + c_1\lambda^2 + c_2\lambda + c_3 = 0\,, \tag{18}$$

with coefficients

$$\begin{aligned} -c_1 &= (1+2k^2)(a_1+a_2+a_3) = m'_1 + m'_2 + m'_3 \\ -c_3 &= 27k^4 a_1 a_2 a_3 = m'_1 m'_2 m'_3 \\ c_2 &= 3k^2(2+k^2)(a_1a_2 + a_2a_3 + a_3a_1) = m'_1m'_2 + m'_2m'_3 + m'_3m'_1\,. \end{aligned} \tag{19}$$

It is clear that $k = 1$ is a special point where

$$3a_i = m'_i\,, \quad i = 1,2,3\,, \tag{20}$$

is a solution; permutation of a_i still leads to a solution. However, our mass matrix (1) with $k = 1$ and with the second and third columns (rows) exchanged is invariant by cyclic permutations which means it is diagonalized by $U_{\rm PMNS} = U_\omega$. This mixing matrix is clearly in contradiction with experiments, a fact that still applies if $k \approx 1$ (for hierarchical m_i). Hence, we need to analyze the cases away from $k = 1$.

Generically we can invert (19) and obtain a_i as functions of m_i and k. Simplification is achieved for generic $k > 0$ by defining

$$\tilde{a}_i \equiv (1+2k^2)a_i\,. \tag{21}$$

Then equations in (19) can be rewritten as

$$\begin{aligned} \tilde{a}_1 + \tilde{a}_2 + \tilde{a}_3 &= m'_1 + m'_2 + m'_3\,, \\ \tilde{a}_1\tilde{a}_2\tilde{a}_3 &= g_3(k) m'_1 m'_2 m'_3\,, \\ \tilde{a}_1\tilde{a}_2 + \tilde{a}_2\tilde{a}_3 + \tilde{a}_3\tilde{a}_1 &= g_2(k)(m'_1m'_2 + m'_2m'_3 + m'_3m'_1)\,. \end{aligned} \tag{22}$$

where

$$g_3(k) \equiv \frac{(1+2k^2)^3}{27k^4}\,, \quad g_2(k) \equiv \frac{(1+2k^2)^2}{3k^2(2+k^2)}\,. \tag{23}$$

The key relation that can be extracted from (22) is that $\tilde{a}_i$ should be now roots of the cubic equation similar to (18) but with coefficients modified by

$$c_1 \to \tilde{c}_1 = c_1\,, \quad c_2 \to \tilde{c}_2 = g_2(k)c_2\,, \quad c_3 \to \tilde{c}_3 = g_3(k)c_3\,. \tag{24}$$

This construction gives $\tilde{a}_i$ as functions of m'_i and k, except for permutations of $\tilde{a}_i$. The solutions (20) for $k = 1$ are modified as $g_2(k), g_3(k)$ differ from unity when $k \neq 1$. Moving away from $k = 1$, both functions increase monotonically (g_2 reaches 4/3 asymptotically as $k \to \infty$).

Now, the distortions caused by $g_{2,3}$ can not be too large because $\tilde{a}_i$ need to be real. To illustrate this point, compare the two polynomials

$$p_1(x) = x^3 - 2.1x^2 + 1.1x\,, \quad p_2(x) = x^3 - 2.1x^2 + 1.2x\,, \tag{25}$$

where the second polynomial differs from the first just by a small deviation in the third coefficient. The first polynomial has three real and distinct roots while the second polynomial has only $x = 0$ as a real root. That can be confirmed by calculating the discriminant of the factored second degree polynomials: $\Delta = (2.1)^2 - 4\times 1.1 = 0.01$ and $\Delta = (2.1)^2 - 4\times 1.2 = -0.39$ for p_1 and p_2 respectively. We can see that two quasi-degenerate eigenvalues are specially sensitive to deviations by k. That is the case of IH with CP parities $(++-)$ or $(+++)$.

The values for k that allow real solutions for $\tilde{a}_i$ can be extracted from the discriminant of the cubic polynomial (18) for which

$$\Delta = \tilde{c}_1^2\tilde{c}_2^2 - 4\tilde{c}_2^3 - 4\tilde{c}_1^3\tilde{c}_3 + 18\tilde{c}_1\tilde{c}_2\tilde{c}_3 - 27\tilde{c}_3^2 \;\geq 0\,. \tag{26}$$

In Fig. 1 we show the values of k as a function of the lightest mass m_0 where the discriminant above is non-negative; we use the current best fit values for the mass differences [9]. The figure in the left (right) correspond to NH (IH) and the various possibilities for CP parities are depicted in different colors. For IH, only the case of CP parities $(-++)$ and $(+-+)$ have wide regions for k for a given mass m_0; the remaining cases has only very narrow ranges of possible k, including $k \approx 1$ which is phenomenologically excluded. The other possible narrow range for k for IH-$(+++)$ (e.g. $k \approx 7$ for $m_0 = 10^{-3}$eV) is also phenomenologically excluded because it leads to $a_1 \approx a_2 \approx a_3$ and two mixing angles are vanishing.

We also illustrate in Fig. 2 the deviations from $\tilde{a}_i = m_i$ when k moves away from $k = 1$. k varies only in the range where the discriminant (26) is non-negative, as shown in Fig. 1. Note that close to the critical values of k ($\Delta = 0$) two (or more) $\tilde{a}_i$ tend to be quasi-degenerate. This is a generic phenomenon.

B. Seeking solutions

After an exhaustive numerical search we conclude that the mass matrix (1) is only compatible with oscillation data for normal hierarchy (NH) and CP parities $(-++)$ and $(+-+)$. The cases

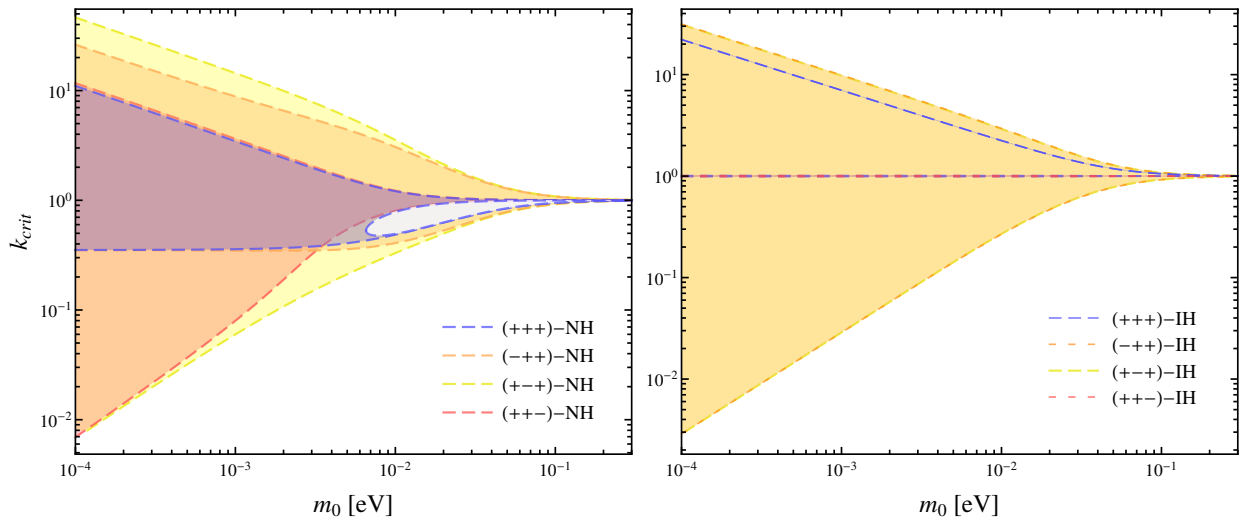

FIG. 1: Left (right): regions in the k-m_1 (k-m_3) plane where solutions for a_i are real for NH (IH). The mass squared differences are fixed to their best fit values of [9]. A hole is only present for the case NH-$(+++)$, the regions for IH-$(-++)$ and IH-$(+-+)$ are almost overlapping, and the regions for IH-$(+++)$ and IH-$(++-)$ can be seen only as lines.

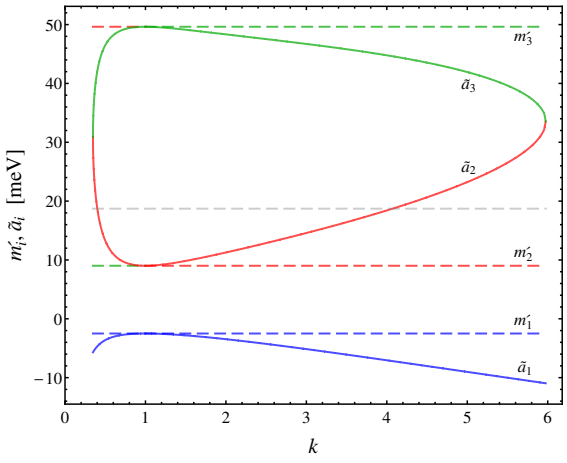

FIG. 2: Solutions of $\tilde{a}_i$ (in solid blue, red and green, respectively) as functions of k and m'_i (in dashed blue, red and green, respectively) for fixed values $(-2.5, 9.014, 49.63)$ meV for m'_i with ordering defined by (30). The gray dashed line corresponds to the average $\frac{1}{3}(m'_1 + m'_2 + m'_3) = \frac{1}{3}(\tilde{a}_1 + \tilde{a}_2 + \tilde{a}_3)$.

of IH and quasi-degenerate masses are excluded. The lightest neutrino mass is restricted to

$$\begin{aligned} (-++): &\quad 1.6\,\text{meV} \lesssim m_1 \lesssim 3\,\text{meV}\,, \\ (+-+): &\quad 3.5\,\text{meV} \lesssim m_1 \lesssim 7.7\,\text{meV}\,. \end{aligned} \tag{27}$$

The predictions for the contribution for neutrinoless double-beta decay coming from light neutrinos is given by

$$\begin{aligned}(-++): &\quad 1.9\,\text{meV} \lesssim |m^{\nu}_{\beta\beta}| \lesssim 2.6\,\text{meV}\,,\\ (+-+): &\quad 1.1\,\text{meV} \lesssim |m^{\nu}_{\beta\beta}| \lesssim 2.05\,\text{meV}\,,\end{aligned} \tag{28}$$

They fall inside the regions denoted by NH-$(-++)$ and NH-$(+-+)$ in Ref. [8]. Note that $m^{\nu}_{\beta\beta} = (M_\nu)^*_{ee}$. For future use, we also list

$$\begin{aligned}(-++): &\quad 26\,\text{meV} \lesssim (M_\nu)_{\mu\tau} \lesssim 28\,\text{meV}\,,\\ (+-+): &\quad 20.5\,\text{meV} \lesssim (M_\nu)_{\mu\tau} \lesssim 23\,\text{meV}\,.\end{aligned} \tag{29}$$

The parameter distribution for the two set of solutions is shown in Fig. 3 for $|a_i|$ as functions of m_1 (left), and k as a function of m_1 (right). The values $\theta_{23} = \pi/4$ and $\delta_{\mathsf{CP}} = \pm\pi/2$ are fixed from symmetry and we only consider values for $\theta_{12}, \theta_{13}, \Delta m^2_{21}$ and Δm^2_{23} within 3-σ of the global fit in Ref. [9] by varying a_i and k independently. Approximate values are obtained from the procedure below.

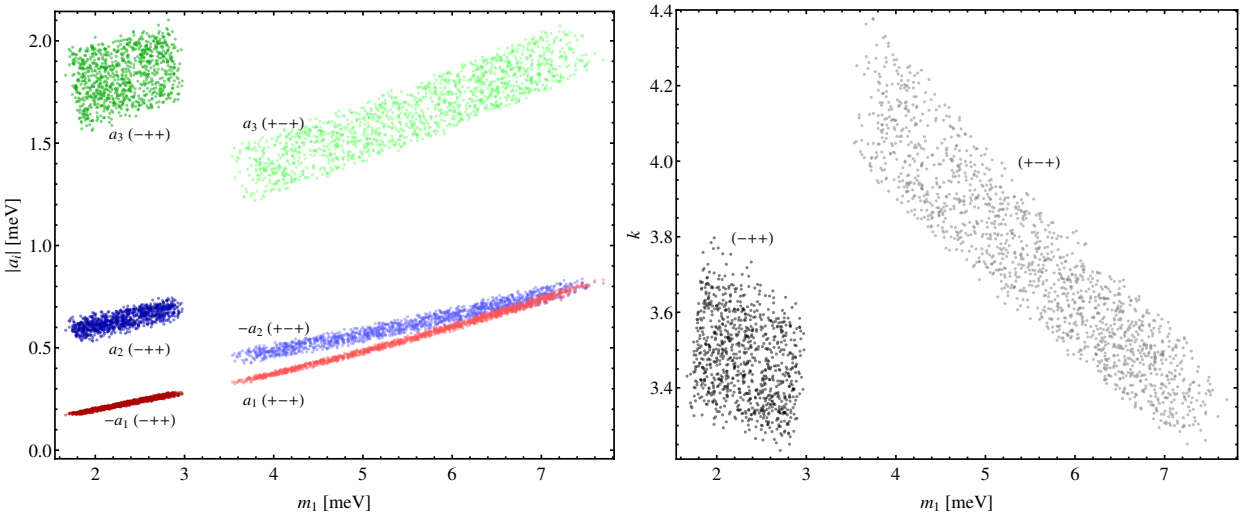

FIG. 3: **Left**: Scatter plot of $|a_i|$ as a function of the lightest mass m_1 (NH) for the two possible CP parities for the light ν_{iL}: $(-++)$ (darker colors) and $(+-+)$ (lighter colors). Other solutions are related by permutations of a_i, cf. (15). The depicted ordering of a_i leads to $\delta_{\mathsf{CP}} = -\pi/2$. **Right**: k as a function of m_1; black dots and gray dots denote the cases $(-++)$ and $(+-+)$ respectively.

We use the following procedure to exclude solutions and search for approximate solutions:

1. For each lightest mass m_0, we find $\tilde{a}_i$ through Eq. (22) (or Eq. (18) with (24)) for a given k, restricted to the range specified by Fig. 1. We keep Δm^2_{12} and Δm^2_{23} fixed to their best fit values of [9]. An illustration of this procedure is given in Fig. 2.

2. Then, we diagonalize (1) to extract the mixing matrix $U = U_{\rm PMNS}$. We adopt the ordering of eigenvectors to satisfy

$$|U_{e1}| > |U_{e2}| > |U_{e3}| \,. \tag{30}$$

The ordering of m_i follows. This means that our mass eigenstates ν_1, ν_2, ν_3 are in the order of decreasing contribution to ν_e (ν_1 contributes the most and so on) and not on a specific mass ordering. This definition explains the color flipping in Fig. 2 for $k < 1$.

3. At last, we check if the mass ordering is correct and if the mixing angles fall inside the 3-σ ranges. An illustration of this step is shown in Fig. 4.

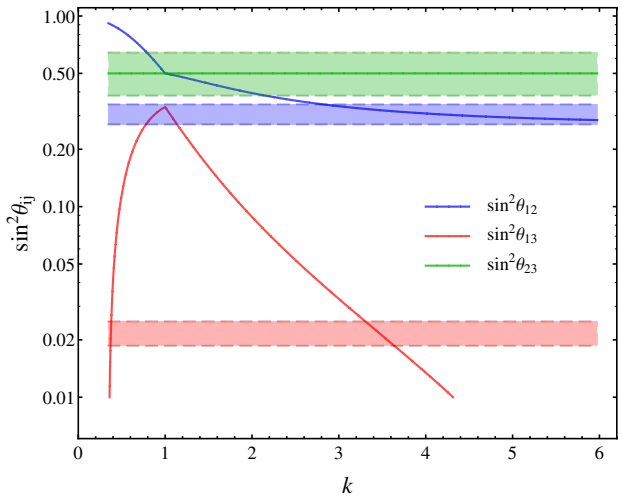

FIG. 4: $\sin^2\theta_{ij}$ as a function of k for $m_1 = 2.5\,\text{meV}$. The colored bands corresponds to the allowed ranges of $\sin^2\theta_{ij}$. We use the same parameters as Fig. 2 and the procedure is explained in Sec. III B.

One remark on this procedure is in order: to correctly fit the oscillation parameters we need that (i) the mixing angles are correct and (ii) the mass ordering is correct. The condition (ii) arises because mass eigenstates ν_i are defined by (30) and mass orderings that do not correspond to NH or IH are excluded. For example, we can read from Fig. 4 that the correct values for both s^2_{12} and s^2_{13} are only achieved for $k \approx 3.5$, as can be also confirmed in Fig. 3. Correct values for s^2_{13} can be also obtained for $k \approx 0.4$ but s^2_{12} as well as the mass ordering in Fig. 2 is not correct: for $k < 1$, ν_e has more contribution from the heaviest state (ν_2 in red) than the second heaviest state (ν_3 in green).

	L_i	l_i	H	N_i	S_i	η	φ_0	φ_1
A_4	$(\mathbf{1},\mathbf{1}',\mathbf{1}'')$	$(\mathbf{1},\mathbf{1}',\mathbf{1}'')$	$\mathbf{1}$	$(\mathbf{1},\mathbf{1}',\mathbf{1}'')$	$\mathbf{3}$	$\mathbf{3}$	$\mathbf{1}$	$\mathbf{1}'$
$\mathbb{Z}_4^D$	1	1	1	1	i	$-i$	-1	-1

IV. EXTENDED SEESAW MODEL

Here we present a low scale seesaw model where the light neutrino mass matrix has the form (1). The model will retain the successful predictions of $\mathrm{U}(1)_{\mu-\tau} \times \mathbb{Z}_2^{\mathsf{CP}}$ [8] for the low energy neutrino observables but additional predictions arise due to the more constrained nature of the group A_4. Two sets of heavy neutrinos – one at the GeV scale and another at the electroweak scale – arise naturally due to the extended seesaw mechanism (ESS) [17]. The combination of lepton flavor numbers $\mathtt{L}_\mu - \mathtt{L}_\tau$ will be approximately conserved in the model.

The flavor symmetry of the model will be $A_4 \times \mathbb{Z}_2^{\mathsf{CP}}$ (CP_2), explained in Sec. II [3]. The SM lepton fields are, however, all singlets of A_4 and only feel the $\mathbb{Z}_3$ subgroup [4], thus entirely avoiding the need of any vev alignment in this sector. An auxiliary $\mathbb{Z}_4^D$ will be also necessary in the neutrino sector. The SM lepton fields are assigned to $L_i \sim l_i \sim (\mathbf{1},\mathbf{1}',\mathbf{1}'')$ while the Higgs doublet H is invariant; $L_i = (\nu_{iL}, l_{iL})^{\mathsf{T}}$ are lepton doublets while $l_i \equiv l_{iR}$ are the charged lepton singlets. Thus CP_2 in (11) can be identified with $\mathsf{CP}^{\mu\tau}$ [8]. There are also two sets of SM singlets (right-handed neutrinos) $N_i \equiv N_{iR}$ and $S_i \equiv S_{iR}$, $i = 1,2,3$, assigned to $(\mathbf{1},\mathbf{1}',\mathbf{1}'')$ and $\mathbf{3}$ respectively. Hence, only the neutrino sector feels the full A_4 group through S_{iR}. We also need complex flavons $\eta \sim \mathbf{3}$ and $\varphi_1 \sim \mathbf{1}'$, and a real $\varphi_0 \sim \mathbf{1}$. The full assignment can be seen in table IV. Additional fields necessary to break $\mathsf{CP}^{\mu\tau}$ in the charged lepton sector are not shown since they can be just adapted from [8].

The charged lepton sector at the electroweak scale will be effectively the SM one [5]

$$-\mathcal{L}^l_{\text{eff}} = y_1 \bar{L}_1 H l_1 + y_2 \bar{L}_2 H l_2 + y_3 \bar{L}_3 H l_3 + h.c.\,, \tag{31}$$

where the $\mathbb{Z}_3$ subgroup is unbroken but $\mathsf{CP}^{\mu\tau}$ is broken at a higher scale by a CP odd scalar [8] so that the correct splitting for $y_\mu = y_2$ and $y_\tau = y_3$ is generated ($y_e = y_1$).

[3] Note that the combined group is a direct product because both factors commute [8].
[4] This contrast with most of the A_4 models for leptons where at least the lepton doublets form triplets [12]
[5] For simplicity we are considering the UV completion by heavy leptons but the multi-Higgs version can be equally considered with the difference that the Higgs that couples to the $\mu - \tau$ flavors is distinct [8].

The neutrino sector at the high scale is given by

$$\begin{aligned}
-\mathcal{L}_\nu = & f_1 \bar{N}_1 \tilde{H}^\dagger L_1 + f_2 \bar{N}_2 \tilde{H}^\dagger L_2 + f_3 \bar{N}_3 \tilde{H}^\dagger L_3 \\
& + f_1'(\bar{S}\eta)_1 N_1^c + f_2'(\bar{S}\eta)_{1'} N_2^c + f_3'(\bar{S}\eta)_{1''} N_3^c \\
& + \tfrac{1}{2} M_{11} \bar{N}_1 N_1^c + M_{23} \bar{N}_2 N_3^c \\
& + \tfrac{1}{2} k_0 \varphi_0 (\bar{S} S^c)_1 + \tfrac{1}{2} k_1 \varphi_1 (\bar{S} S^c)_{1''} + \tfrac{1}{2} k_1^* \varphi_1^* (\bar{S} S^c)_{1'} \\
& + h.c.,
\end{aligned} \tag{32}$$

where we have defined singlet combinations of two triplets of A_4 as

$$\begin{aligned}
(xy)_1 &\equiv x_1 y_1 + x_2 y_2 + x_3 y_3 \,, \\
(xy)_{1'} &\equiv x_1 y_1 + x_2 y_2 \omega^2 + x_3 y_3 \omega \,, \\
(xy)_{1''} &\equiv x_1 y_1 + x_2 y_2 \omega + x_3 y_3 \omega^2 \,.
\end{aligned} \tag{33}$$

Note that $\mathsf{CP}^{\mu\tau}$ acts as

$$\begin{aligned}
\mathsf{CP}^{\mu\tau}: \quad & L_1 \to L_1^{cp}, \quad L_2 \to L_3^{cp}, \quad L_3 \to L_2^{cp}, \\
& H \to H^*, \quad S_i \to S_i^{cp}, \quad \eta_i \to \eta_i^*, \\
& \varphi_0 \to \varphi_0, \quad \varphi_1 \to \varphi_1 \,,
\end{aligned} \tag{34}$$

and l_i and N_i transform like L_i and ψ^{cp} denotes the usual CP conjugate of the chiral fermion ψ. Therefore, $f_1, f_1', M_{11}, M_{23}, k_0$ are real and $f_3 = f_2^*$, $f_3'^* = f_2'$ due to $\mathsf{CP}^{\mu\tau}$. The parameters $f_{2,3}, f_{2,3}'$ can be further chosen real and positive by rephasing $L_{2,3}$ and $N_{2,3}$.

The mass matrix for (ν_{iL}, N_i^c, S_i^c) after EWSB will be

$$\mathbb{M} = \begin{pmatrix} \mathbf{0} & M_D^{\mathsf{T}} \\ M_D & M_R \end{pmatrix} = \begin{pmatrix} \mathbf{0} & m_D^{\mathsf{T}} & \mathbf{0} \\ m_D & M_N & \Lambda^{\mathsf{T}} \\ \mathbf{0} & \Lambda & \mu \end{pmatrix} , \tag{35}$$

where

$$\begin{aligned}
m_D &= \mathrm{diag}(m_{D_{ii}}) = \frac{v}{\sqrt{2}} \,\mathrm{diag}(f_1, f_2, f_3) \,, \\
\Lambda &= \mathrm{diag}(u_1, u_2, u_3) \sqrt{3} U_\omega^* \,\mathrm{diag}(f_1', f_2', f_3') \,, \\
M_N &= \begin{pmatrix} M_{11} & & \\ & & M_{23} \\ & M_{23} & \end{pmatrix} , \\
\mu &= \mathrm{diag}(\mu_1, \mu_2, \mu_3) \,,
\end{aligned} \tag{36}$$

where

$$U_\omega \equiv \frac{1}{\sqrt{3}} \begin{pmatrix} 1 & 1 & 1 \\ 1 & \omega & \omega^2 \\ 1 & \omega^2 & \omega \end{pmatrix} . \tag{37}$$

In this model, we are considering that $\varphi_{0,1}$ acquire very small vevs which lead to the real Majorana masses μ_i for S_i and also

$$\langle \eta_i \rangle = u_i \,, \quad \text{all real.} \tag{38}$$

We justify the hierarchy of vevs in appendix B.

Considering that M_N is composed of bare masses, the ESS limit is naturally achieved [17]: $M_N \gg \{\Lambda, m_D\} \gg \mu$ and also $\mu \ll \Lambda^2/M_N$. We can see that there are two sources of lepton number violation (LNV) in (32) [6]: (a) large scales M_N and (b) low scales $\mu_i \sim \langle \varphi_{0,1} \rangle$.

At tree level and leading order we obtain

$$\begin{aligned} \nu_i : &\quad M_\nu = m_D^{\mathsf{T}} \Lambda^{-1} \mu (\Lambda^{\mathsf{T}})^{-1} m_D \,, \\ S_i^c : &\quad M_S = -\Lambda M_N^{-1} \Lambda^{\mathsf{T}} \,, \\ N_i^c : &\quad M_N \,, \end{aligned} \tag{39}$$

with light-heavy mixing

$$\begin{aligned} \theta_{\nu S}^* &= m_D^{\mathsf{T}} \Lambda^{-1} \,, \\ \theta_{\nu N}^* &= m_D^{\mathsf{T}} M_N^{-1} \,. \end{aligned} \tag{40}$$

Additional mixings can be seen in appendix A. We can see that the small LNV scale μ only enters M_ν while the large LNV scale M_N contributes only to heavier masses. Given that the mass matrix for the heavier states N_i are approximately unchanged, we can define

$$M_{N_1} \equiv M_{11}, \quad M_{N_2} = M_{N_3} \equiv M_{23}, \tag{41}$$

assuming positive quantities. The leading correction can be seen in appendix A.

Explicitly, the light neutrino mass matrix is

$$M_\nu = \tfrac{1}{3} \operatorname{diag}(m_{D_{ii}}/f_i') U_\omega \operatorname{diag}(\mu_i/u_i^2) U_\omega \operatorname{diag}(m_{D_{ii}}/f_i') \,, \tag{42}$$

which has the desired form (1) with

$$a_i = \tfrac{1}{9} \mu_i \frac{m_{D_{11}}^2}{u_i^2 f_1'^2} \,, \quad k = \frac{|m_{D_{22}} f_1'|}{|m_{D_{11}} f_2'|} \,. \tag{43}$$

[6] If $\mathtt{L}(N_i) = \mathtt{L}(L_i) = -\mathtt{L}(S_i) = 1$.

We have used the shorthand $m_{D_{11}} \equiv f_1 v/\sqrt{2}$; cf. (36). Fitting of the light neutrino parameters in Fig. 3 implies

$$\begin{aligned} |a_i| &\approx 0.2 - 2.1\,\text{meV}\,, \\ k &\approx 3.2 - 4.4\,. \end{aligned} \tag{44}$$

Also, the sign change of one of the a_i needs to be generated by μ_i and not by u_i^2 which is always positive.

Although frequently the heavier states N_i are chosen to lie above the TeV scale [17, 18], in our case (i) negligible one-loop contribution for light neutrino masses, (ii) validity of the ESS approximation and (iii) BBN constraints will essentially restrict M_N to the electroweak scale; see Sec. VI and (70) for a benchmark point.

V. APPROXIMATE $\mathrm{U}(1)_{\mu-\tau}$ LIMIT

We consider first the limit where $\mathbb{Z}_3$ of A_4 is only broken by the small quantities in μ. This means that below the scale of $\langle\eta\rangle$, $\mathbb{Z}_3$ is only broken by light neutrinos masses. This approximate $\mathbb{Z}_3$ symmetry corresponds to the *lepton flavor triality* (LFT) [19] where lepton fields carry the discrete charges

$$\text{LFT}: \quad L_i \sim l_i \sim N_i \sim S_i'^c \sim (1, \omega, \omega^2)\,; \tag{45}$$

S_i' is related to S_i by change of basis $S_i^c = (U_\omega)_{ij} S_j'^c$.

The heavy vevs of η conserve LFT when

$$\langle\eta_i\rangle = u_i \approx u_0(1,1,1)\,. \tag{46}$$

This feature is justified in appendix B. In this case, after $\eta_i \to \langle\eta_i\rangle$ and in the limit $k_1 \to 0$, the Lagrangian (32) is in fact invariant by the continuous version of (45) with charges [8]

$$\mathrm{U}(1)_{\mu-\tau}: \quad L_i \sim l_i \sim N_i \sim S_i'^c \sim (0, 1, -1)\,. \tag{47}$$

It corresponds to the combination $\mathtt{L}_\mu - \mathtt{L}_\tau$ of family lepton numbers. The approximate conservation of $\mathrm{U}(1)_{\mu-\tau}$ will lead to a number of consequences.

In this limit the mass matrix (39) and mixing (40) of the heavy neutrinos S_i yield

$$\begin{aligned} M_S &= -\tfrac{1}{3}\begin{pmatrix} M_{S_1}+2M_{S_2} & M_{S_1}-M_{S_2} & M_{S_1}-M_{S_2} \\ \star & M_{S_1}+2M_{S_2} & M_{S_1}-M_{S_2} \\ \star & \star & M_{S_1}+2M_{S_2} \end{pmatrix}, \\ \theta^*_{\nu S} &= \frac{m_{D_{11}}}{\sqrt{3}f_1' u_0}\begin{pmatrix} 1 & & \\ & k & \\ & & k \end{pmatrix} U_\omega \,, \end{aligned} \tag{48}$$

where the masses read [7]

$$M_{S_1} \equiv \frac{(\sqrt{3}u_0 f_1')^2}{M_{N_1}}\,, \quad M_{S_{2,3}} \equiv \frac{(\sqrt{3}u_0|f_2'|)^2}{M_{N_2}}\,. \tag{49}$$

These relations allows us to trade $f_1' u_0$ and $f_2' u_0 = f_3' u_0$ for physical masses:

$$|\sqrt{3}f_1' u_0| = \sqrt{M_{S_1} M_{N_1}}\,, \quad |\sqrt{3}f_2' u_0| = \sqrt{M_{S_2} M_{N_2}}\,. \tag{50}$$

The mass matrix M_S is invariant by cyclic permutations and then $(1,1,1)$ is an eigenvector. We can diagonalize it by

$$V_S^* = U_\omega^*(-i)U_{23}^*\,. \tag{51}$$

giving

$$V_S^{\mathsf{T}} M_S V_S = \mathrm{diag}(M_{S_1}, M_{S_2}, M_{S_3})\,. \tag{52}$$

The matrix U_{23} was defined in (17). Therefore, S_1 is a Majorana fermion of $\mathrm{U}(1)_{\mu-\tau}$ charge 0 and $S_{2,3}$ are degenerate Majorana fermions that form a (pseudo-)Dirac pair of fields with charge ± 1. The latter implies that LNV effects induced by $S_{2,3}$ exchange will vanish in this limit.

The active-sterile ν-S mixing reduces to

$$(\theta_{\nu S} V_S)^* = (-i)\frac{m_{D_{11}}}{\sqrt{3}u_0 f_1'}\,\mathrm{diag}(1,k,k)\begin{pmatrix} 1 & 0 & 0 \\ 0 & \frac{1}{\sqrt{2}} & -\frac{i}{\sqrt{2}} \\ 0 & \frac{1}{\sqrt{2}} & \frac{i}{\sqrt{2}} \end{pmatrix}. \tag{53}$$

It is important to note that in this approximation

$$(\theta_{\nu S} V_S)_{ei} = 0\,, \text{ for } i = 2,3, \tag{54}$$

and the electron flavor is only coupled to S_1.

[7] We keep using the same name S_i for the heavy neutrino fields although they have a small component of ν_{iL}^c and N_{iR}.

VI. ONE-LOOP CONTRIBUTIONS AND BBN CONSTRAINTS

Now we should compute the one-loop contributions to light neutrino masses. When the lightest heavy RHN mass lies below 100 MeV, the one-loop contributions to $0\nu2\beta$ can be sizable [20], although such a sterile neutrinos are severely constrained by cosmological data [21]. Heavy neutrinos with electroweak scale masses can still induce sizable contributions [18, 22] and the dominant (and finite) one comes from light neutrino self-energies with higgs or Z exchange [23–25].

We can write the self-energy contribution as

$$M_\nu^{\text{1-l}} = \frac{1}{(4\pi v)^2} M_D^{\mathsf{T}} \Big(M_R^{-1} F(M_R M_R^\dagger) + F(M_R M_R^\dagger) M_R^{-1} \Big) M_D \,, \tag{55}$$

where the loop function $F(x)$ is given by

$$F(x) \equiv \frac{x}{2} \left[3\, \frac{\ln(x/M_Z^2)}{x/M_Z^2 - 1} + \frac{\ln(x/M_h^2)}{x/M_h^2 - 1} \right] , \tag{56}$$

with M_Z and M_h being the Z and Higgs boson masses, respectively; $v = 246\,\text{GeV}$ is the electroweak scale. This contribution should be added to the tree-level contribution (42) coming from the ESS mechanism. We should note that heavy neutrinos masses M_R at the electroweak scale leads to a contribution (55) functionally similar to the tree-level contribution M_D^2/M_R, but smaller only by the loop factor $1/16\pi^2$ [23] [notice $F\big((100\,\text{GeV})^2\big)/v^2 \approx 1.5$]. Therefore, the one-loop contribution in the ESS mechanism can be possibly large since the cancellation that occurs in the tree-level mass matrix is not expected to carry over to the one-loop contribution.

We can adapt the one-loop contribution for generic type-I seesaw (55) to the extended seesaw with mass matrix (35) as

$$M_\nu^{\text{1-l}} = \frac{1}{(4\pi v)^2} m_D^{\mathsf{T}} \Big\{ M_N^{-1} \Lambda^{\mathsf{T}} V_S\, \hat{M}_S^{-1} 2F(\hat{M}_S^2) V_S^{\mathsf{T}} \Lambda M_N^{-1} + V_N\, \hat{M}_N^{-1} 2F(\hat{M}_N^2) V_N^{\mathsf{T}} \Big\} m_D \,. \tag{57}$$

We have first block diagonalized M_R (see appendix A) and then used the basis where M_S and M_N is diagonal ($\hat{M}_S$ and $\hat{M}_N$). It is also possible to write the expression in terms of the light-heavy mixing angles as

$$M_\nu^{\text{1-l}} = \frac{1}{(4\pi v)^2} \Big\{ (\theta_{\nu S} V_S)^*\, \hat{M}_S\, 2F(\hat{M}_S^2) (\theta_{\nu S} V_S)^\dagger + (\theta_{\nu N} V_N)^*\, \hat{M}_N\, 2F(\hat{M}_N^2) (\theta_{\nu N} V_N)^\dagger \Big\} . \tag{58}$$

We can see that generically the contribution from the heavier states N_i *dominates* over the contribution from S_i because the smaller mixing angle $\theta_{\nu N}^2/\theta_{\nu S}^2 \sim \Lambda^2/M_N^2$ is compensated by $M_N/M_S \sim M_N^2/\Lambda^2$ and $F(x)$ grows with x.

For our purposes, it is useful to define the adimensional function $g(x)$ as

$$g(M_i/100\,\text{GeV}) \equiv \frac{2F(M_i^2)}{M_i \times 100\,\text{GeV}} \,. \tag{59}$$

A slightly different definition can be seen in [26]. This function peaks at the electroweak scale $M_i \approx 93.3\,\text{GeV}$ with maximum 3.64 and decreases away from the peak with rate slower than M_i^{-1} for $M_i \gtrsim 100\,\text{GeV}$; see behaviour in Fig. 5. This function allows us to rewrite (57) as

$$M_\nu^{\text{1-l}} = \frac{100\,\text{GeV}}{(4\pi v)^2} m_D^{\mathsf{T}} \Big\{ M_N^{-1} \Lambda^{\mathsf{T}} V_S\, g(\hat{X}_S) V_S^{\mathsf{T}} \Lambda M_N^{-1} + V_N\, g(\hat{X}_N) V_N^{\mathsf{T}} \Big\} m_D\,. \tag{60}$$

We have used the shorthand $\hat{X}_S \equiv \text{diag}(M_{S_i})/100\,\text{GeV}$ and similarly for $\hat{X}_N$.

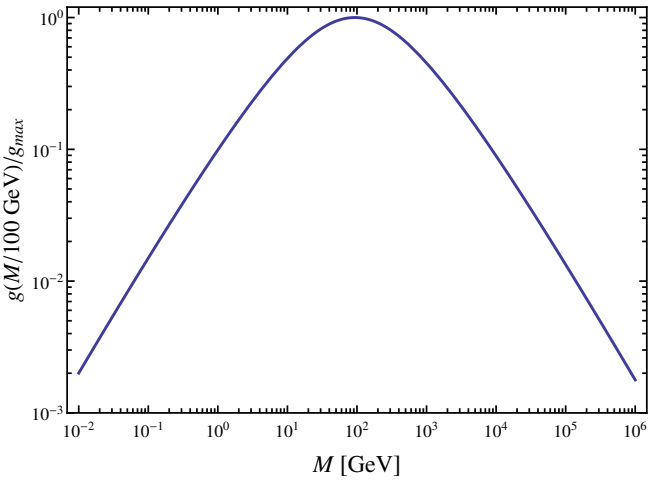

FIG. 5: Plot of the function in (59) where $g_{\text{max}} = 3.63547$ and the maximum occurs at $M \approx 93.3\,\text{GeV}$.

Computing (60) in our model in the $\text{U}(1)_{\mu-\tau}$ symmetric limit, we obtain the texture

$$M_\nu^{\text{1-l}} = \begin{pmatrix} \star & 0 & 0 \\ 0 & 0 & \star \\ 0 & \star & 0 \end{pmatrix}, \tag{61}$$

whose nonzero entries correspond to $\mathtt{L}_\mu - \mathtt{L}_\tau = 0$. Explicitly,

$$\begin{aligned} (M_\nu^{\text{1-l}})_{ee} &\approx 10\,\text{keV} \times \frac{m_{D_{11}}^2}{\text{GeV}^2} \Big[-\frac{g(x_1)}{M_{N_1}/M_{S_1}} + g\Big(\frac{M_{N_1}}{M_{S_1}} x_1\Big) \Big], \\ (M_\nu^{\text{1-l}})_{\mu\tau} &\approx 10\,\text{keV} \times \frac{m_{D_{22}}^2}{\text{GeV}^2} \Big[-\frac{g(x_2)}{M_{N_2}/M_{S_2}} + g\Big(\frac{M_{N_2}}{M_{S_2}} x_2\Big) \Big], \end{aligned} \tag{62}$$

where $x_i \equiv M_{S_i}/100\,\text{GeV}$. We have used Eqs. (36), (51) and $V_N = U_{23}$. We note that indeed the one-loop contribution can lead to an unacceptably large contribution. For example, for $m_D \sim 1\,\text{GeV}, M_N \sim 10\,\text{TeV}, M_S \sim 100\,\text{GeV}$, the one-loop contribution leads to a few keV. From Fig. 5 we also see that to lower the contributions from (62) to acceptable values by increasing M_N requires very large values of the order of $10^7\,\text{GeV}$. Therefore, to have TeV scale (or lower) right-handed neutrinos, we need to lower the scale of m_D or arrange some cancellation between either the various

one-loop contributions or between the tree and one-loop ones [25]. We consider this possibility unappealing and do not pursue it any further.

In order to preserve our predictions of Sec. III we confine ourselves to the case where the loop induced contributions (62) are negligible compared to the tree level ones in (1). To visualize the possible regions in parameter space, we show in Fig. 6 the regions (blue) in the M_{N_1}-$m_{D_{11}}$ plane (left) and M_{N_2}-$m_{D_{22}}$ plane (right) where the one-loop contribution is at most 10% of the tree-level contribution for the ee (left) and $\mu\tau$ (right) entries. For definiteness we fix the tree-level values to

$$\begin{aligned} (M_\nu^{\text{tree}})_{ee} &= 2\,\text{meV}, \quad R_{N_1} \equiv M_{N_1}/M_{S_1} = 10^2\,, \\ (M_\nu^{\text{tree}})_{\mu\tau} &= 24\,\text{meV}\,, \quad R_{N_2} \equiv M_{N_2}/M_{S_2} = 10^2\,. \end{aligned} \tag{63}$$

These values are in agreement with (28) and (29). We choose to plot the dependence on M_{N_i} because the one-loop contributions depend dominantly on M_{N_i} (rather than on the lighter M_{S_i}) in the ESS approximation. For example, if we increase the ratios R_{N_i}, the blue regions shrinks down only slightly for large M_{N_i}. For completeness, we also show the curves for unit ratio (dashed).

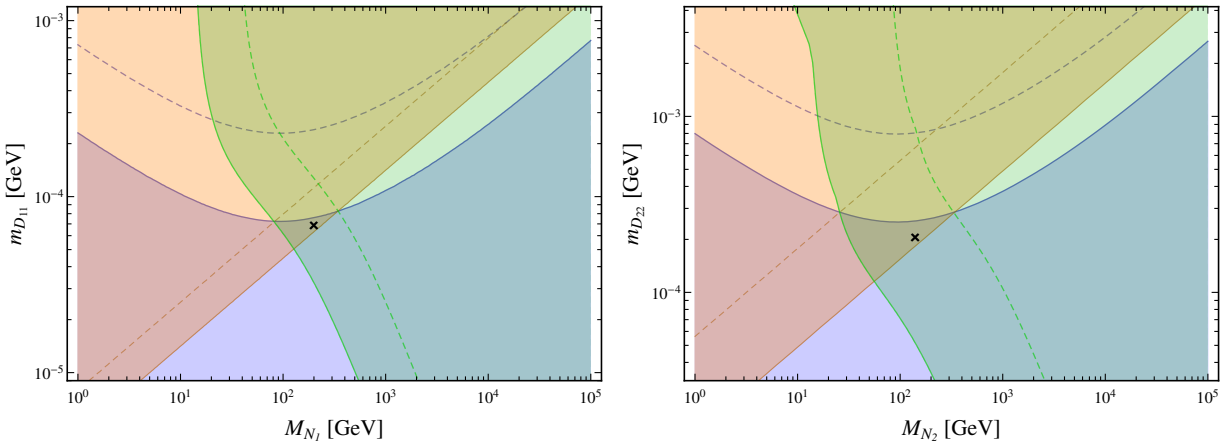

FIG. 6: The blue regions satisfy $|(M_\nu^{\text{1-l}})_{ee}|/|(M_\nu^{\text{tree}})_{ee}| \leq 0.1$ (left) or $|(M_\nu^{\text{1-l}})_{\mu\tau}|/|(M_\nu^{\text{tree}})_{\mu\tau}| \leq 0.1$ (right) with the reference values (63). The blue dashed curves obey unit ratios. The points inside the orange regions are the ones necessary to fit the ee (left) or $\mu\tau$ (right) tree-level entries of the light neutrino mass matrix through (64) or (65) restricted to (66) and (63). The orange dashed curves correspond to the subset of points for $R_{\mu 1} = 0.03$ (left) and $R_{\mu 2} = 0.076$ (right). The green regions cover the points where $\tau_{S_1} \leq 0.1$ (left) or $\tau_{S_2} \leq 0.1$ (right) for $R_{N_1} = R_{N_2} = 100$. The green dashed curves yields the life-time of 0.1 s but with $R_{N_1} = 270$ (left) or $R_{N_2} = 400$ (right). The crosses mark the benchmark points in (70). See text for details.

The next step is to ensure that the tree-level contribution themselves – as they *depend* on the model parameters as in (43) – lie in the necessary ranges of (28) and (29) (also Fig. 3). For that

purpose, we rewrite the sum of all relations for a_i in (43) as

$$\left(\frac{m_{D_{11}}}{10\text{keV}}\right)^2 \left(\frac{100\,\text{GeV}}{M_{N_1}}\right) \left(\frac{\bar{\mu}_i}{M_{S_1}}\right) = \frac{|(M_\nu^{\text{tree}})_{ee}|}{\text{meV}}\,, \tag{64}$$

where $\bar{\mu}_i \equiv \sum_i \mu_i/3$. We have also used (50) to eliminate $f_1' u_0$. An analogous relation is valid for the $\mu\tau$ entry:

$$\left(\frac{M_{D_{22}}}{10\text{keV}}\right)^2 \left(\frac{100\,\text{GeV}}{M_{N_2}}\right) \left(\frac{\bar{\mu}_i}{M_{S_2}}\right) = \frac{|(M_\nu^{\text{tree}})_{\mu\tau}|}{\text{meV}}\,. \tag{65}$$

As $\bar{\mu}_i \ll M_{S_1}$ in order to satisfy the ESS approximation, we require

$$R_{\mu 1} \equiv \frac{\bar{\mu}_i}{M_{S_1}} \leq 0.1 \quad \text{and} \quad R_{\mu 2} \equiv \frac{\bar{\mu}_i}{M_{S_2}} \leq 0.1\,. \tag{66}$$

These conditions define allowed regions for M_{N_1}-$m_{D_{11}}$ and M_{N_2}-$m_{D_{22}}$ which are shown as orange regions in Fig. 6. We also show in dashed orange curves the values where the above ratios assume the values $R_{\mu 1} = 0.03$ (left) and $R_{\mu 2} = 0.0076$ (right). We use the same reference values in (63).

The conclusion is that the overlapping (allowed) regions impose upper bounds on the heavy RHN states:

$$M_{N_1}, M_{N_2} \lesssim 340\,\text{GeV}\,. \tag{67}$$

This constraint puts the RHN states S_i at the GeV scale. We also note that had we allowed $M_\nu^{\text{1-l}} \sim M_\nu^{\text{tree}}$, M_{N_1} would be unbounded but restricted to a narrow band $M_{D_{11}}^2/M_{N_1} \sim 10^{-11}\,\text{GeV}$ for $M_{N_1} \gtrsim 1\,\text{TeV}$. A similar consideration applies to M_{N_2}.

As the last constraint, we note that $m_{D_{ii}}$ can not be pushed to arbitrarily low values because it necessarily makes the lighter BSM states S_i to be very long lived [8]. In order to not spoil the successful prediction of Big Bang nucleosinthesis (BBN), we require that the life-times of all the BSM states do not exceed 0.1 s. It is enough to require that for the lighter S_i states. As their masses lie at the GeV scale or lower, the main decay modes involve W or Z exchange through active-sterile mixing with decay into light neutrinos, electrons or pions [30]; see appendix C for more details. The allowed regions are shown in green in Fig. 6 where the border is determined by the fixed $N - S$ ratios of (63); the interior refers to $R_{N_1} > 10^2$ (left) or $R_{N_2} > 10^2$ (right) in accordance to the ESS approximation. For completeness, we also show as dashed green curves the points where $\tau = 0.1\,\text{s}$ and $R_{N_1} = 270$ (left) or $R_{N_2} = 400$ (right).

The combination of all the constraints discussed above, leads to the overlapping regions of Fig. 6. The parameters are restricted to the values listed in Table I. The restriction means that points

[8] We assume all the scalars to be heavier than S_i.

outside the overlapping region violate some constraint above for the reference values (63).[9] Points inside the overlapping regions need to be further checked for all the constraints as they depend on other parameters not shown in the figures. Moreover, the parameters are not all independent as one ratio is fixed through (44) and

$$\frac{m_{D_{22}}}{m_{D_{11}}}\frac{M_{N_1}}{M_{N_2}}\frac{\sqrt{R_{N_2}}}{\sqrt{R_{N_1}}} = k\,. \tag{68}$$

To use tree-level values different from (63) but restricted to (28) and (29), we just need to reread Fig. 6 with the vertical axis relabeled as

$$\begin{aligned} m_{D_{11}} &\to m_{D_{11}}\sqrt{\frac{2\,\mathrm{meV}}{(M_\nu)^{\mathrm{tree}}_{ee}}}\,, \\ m_{D_{22}} &\to m_{D_{22}}\sqrt{\frac{24\,\mathrm{meV}}{(M_\nu)^{\mathrm{tree}}_{\mu\tau}}}\,. \end{aligned} \tag{69}$$

That is possible because all the defining relations, Eqs. (62) (64), (65) and the active-sterile mixing $\theta_{\nu S}$ in the decay rates (ap. C) depends on $m^2_{D_{11}}$ or $m^2_{D_{22}}$. For the same reason, the blue and orange curves of the right figure of Fig. 6 are identical to the ones on the left if we identify $m_{D_{22}} = m_{D_{11}}\sqrt{24/2}$, where $\sqrt{24/2}$ is basically the factor k.

$m_{D_{11}}/10^{-5}\,\mathrm{GeV}$	5 – 8	$m_{D_{22}}/10^{-5}\,\mathrm{GeV}$	12 – 28
M_{N_1}/GeV	80 – 340	M_{N_2}/GeV	25 – 340
M_{N_1}/M_{S_1}	100 – 270	M_{N_2}/M_{S_2}	100 – 400
$\bar{\mu}_i/M_{S_1}$	0.03 – 0.1	$\bar{\mu}_i/M_{S_2}$	0.0076 – 0.1

TABLE I: Approximate parameter values extracted from Fig. 6.

As an example, the following values pass all the constraints and are also marked in Fig. 6 by crosses:

$$\begin{aligned} &M_{D_{11}} = 7\times10^{-5}\,\mathrm{GeV}\,, \quad M_{N_1} = 200\,\mathrm{GeV}\,, \quad M_{S_1} = 1.33\,\mathrm{GeV}\,, \quad \bar{\mu}_i \sim 100\,\mathrm{MeV}\,, \\ &M_{D_{22}} = 2.1\times10^{-4}\,\mathrm{GeV}\,, \quad M_{N_2} = 100\,\mathrm{GeV}\,, \quad M_{S_2} = 1\,\mathrm{GeV}. \end{aligned} \tag{70}$$

The intermediate scales $\sqrt{3}u_0 f_1' \approx 16\,\mathrm{GeV}$ and $\sqrt{3}u_0 f_2' = 10\,\mathrm{GeV}$ can be obtained from (50). They set a lower bound for the scales $\langle\eta_i\rangle \sim u_0 \gtrsim 10\,\mathrm{GeV}$ and $\langle\varphi_0\rangle \sim \langle\varphi_1\rangle \gtrsim \mu_i \sim 0.1\,\mathrm{GeV}$ while the

[9] The actual green regions may lie slightly to the left for two reasons: (i) we only include the dominant decay modes for S_i listed in appendix C and (ii) the strict life-time limit for successful BBN may be slightly relaxed depending on the details of the model at the BBN era [27].

masses can be chosen $M_\eta \sim u_0 \gtrsim M_\varphi \sim 10\,\text{GeV}$. Using the values in (70) as a benchmark, we plot in Fig. 7 the ratio of the one-loop contribution to the tree-level value of $|m^\nu_{\beta\beta}| = |(M^{\text{tree}}_\nu)^*_{ee}| = 2\,\text{meV}$ where now we vary M_{S_1} and rescale M_{N_1} simultaneously by fixing $R_{N_1} = 150$. For the benchmark values (70), the one-loop contribution is indeed less than 10% of the tree-level value. We also show the ratio of the life-time to the limit of 0.1 s (solid gray) and confirm that M_{S_1} needs to be larger than around 1 GeV.

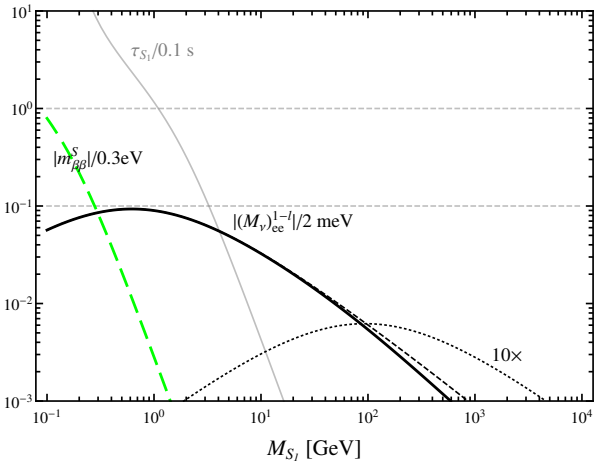

FIG. 7: Ratio of one-loop to tree-level contribution (2 meV) to the ee entry ($0\nu2\beta$ parameter) of the light neutrino mass matrix (solid black) as a function of M_{S_1} (M_{N_1} scales with M_{S_1} through $M_{N_1} = R_{N_1} M_{S_1}$). We also show the contribution coming only from N_1 (dashed) and S_1 (dotted) exchange; the latter is multiplied by 10 for visualization. The contribution for $0\nu2\beta$ parameter from S_1 exchange (green dashed) relative to the limit 0.3 eV is shown as well; we use the expression in (79). The solid gray curve shows the life-time for S_1 relative to 0.1 s. The other parameters are fixed as $m_{D_{11}} = 7 \times 10^{-5}\,\text{GeV}$ and $R_{N_1} = 150$.

Finally, we can estimate the amount of cancellation that is built-in in our ESS mechanism implementation. Rewriting (64) in the form of the naive seesaw relation,

$$|(M^{\text{tree}}_\nu)_{ee}| = \epsilon_{ee} \frac{m^2_{D_{11}}}{M_{S_1}}\,, \tag{71}$$

we extract

$$\epsilon_{ee} = \frac{\bar{\mu}_i}{M_{N_1}} \approx 10^{-3} - 10^{-4}\,, \tag{72}$$

if we use Table I. Analogously, for the $\mu\tau$ entry, we obtain $\epsilon_{\mu\tau} \approx 10^{-3} - 2 \times 10^{-6}$. These values are in agreement with the radiative stability conditions discussed in Ref. [18] that estimated a lower bound of $\epsilon > 10^{-6}$ for a GeV scale right-handed neutrino mass.

VII. OTHER PHENOMENOLOGICAL CONSTRAINTS AND $\mathrm{U}(1)_{\mu-\tau}$ BREAKING

We analyze here other phenomenological constraints coming from the existence of GeV scale heavy neutrino S_i with mixing with the light neutrinos at the order of

$$\begin{aligned} |(\theta V_S)_{e1}|^2 &= \left(\frac{m_{D_{11}}}{\sqrt{3}u_0 f_1'}\right)^2 = \frac{m_{D_{11}}^2}{M_{S_1} M_{N_1}} \\ &= 10^{-12} \times \left(\frac{m_{D_{11}}}{10\,\mathrm{keV}}\right)^2 \left(\frac{100\,\mathrm{GeV}}{M_{N_1}}\right) \left(\frac{1\,\mathrm{GeV}}{M_{S_1}}\right) . \end{aligned} \tag{73}$$

where we have used (50) and simplified the notation for $\theta_{\nu S} V_S$. For the values (70),

$$|(\theta V_S)_{e1}|^2 = \frac{m_{D_{11}}^2}{M_{S_1} M_{N_1}} \sim \frac{(7\times 10^{-5}\,\mathrm{GeV})^2}{200\,\mathrm{GeV}\times 1.33\,\mathrm{GeV}} \sim 2\times 10^{-11} . \tag{74}$$

The other mixing angles are either of the same order or vanishing in the limit of $\mathrm{U}(1)_{\mu-\tau}$ conservation; cf. (53). At the same time, the Yukawa couplings to the RHN in our model are even more suppressed,

$$\begin{aligned} f_1 &\sim \frac{7\times 10^{-5}\,\mathrm{GeV}}{174\,\mathrm{GeV}} \sim 4\times 10^{-7} , \\ f_{2,3} &\sim \frac{2.1\times 10^{-4}\,\mathrm{GeV}}{174\,\mathrm{GeV}} \sim 10^{-6} . \end{aligned} \tag{75}$$

They are smaller than the electron Yukawa coupling and thus the Higgs coupling to the RHN are very much suppressed (their are smaller than the mixing $\theta_{\nu S}$). Hence, the main interactions of the RHN to the SM fields occur through active-sterile mixing in (73).

However, it is clear that indirect detection constraints such as lepton universality violation or electroweak precision tests are not able to restrict or probe such a small mixing angles [28, 29]. They are also unobservable through direct detection in meson decays [28–30] or in colliders [31]. Note that this scenario contrasts with models where Higgsses charged under $\mathbb{Z}_3$ [or $\mathrm{U}(1)_{\mu-\tau}$] may induce large lepton flavor violating Higgs decays [32].

For the same reason, lepton flavor violation (LFV) constraints are very weak in our model. The suppression is even larger because LFV processes such as $\mu \to e\gamma$ or $\mu \to eee$ are forbidden in the limit of $\mathrm{U}(1)_{\mu-\tau}$ conservation. One can also see this in (53) as $(\theta V_S)_{ei}(\theta V_S)^*_{\mu i}$ always vanish. Being a larger group, $\mathrm{U}(1)_{\mu-\tau}$ is more constraining than lepton flavor triality [19] and the former only allows $\tau^- \to \mu^+ e^- e^-$. However, when this process is mediated only by heavy neutrinos, it occurs through box diagrams that are very much suppressed [33]. These conclusions are not modified when $\mathrm{U}(1)_{\mu-\tau}$ breaking effects are considered. See appendix D.

At last, we can analyze the limits coming from neutrinoless double beta decay, which are the strongest involving the mixing with the electron flavor. Since the active-sterile mixings are all

vanishing or of the same order in the $\mathrm{U}(1)_{\mu-\tau}$ symmetry limit, cf. (53), we expect that this process will pose the strongest constraint on the mixings.

The half-life of the process is proportional to [18, 28]

$$\frac{1}{T^{0\nu}_{1/2}} \propto \left| \frac{m^{\nu}_{\beta\beta}}{\langle p^2 \rangle} + \sum_{i=1}^{n_s} \frac{(\theta V)^2_{ek} M_i}{\langle p^2 \rangle - M_i^2} \right|^2 , \tag{76}$$

where $\langle p^2 \rangle \sim -(200\,\mathrm{MeV})^2$ quantifies the effective momentum transfer inside the nucleus and M_i represent the masses of the additional heavy neutrino states that mixes with the three active ones. The light neutrino contribution depends on

$$m^{\nu}_{\beta\beta} \equiv \sum_i U^2_{ei} m_i \,, \tag{77}$$

with contributions arising from tree and loop contributions

$$(m^{\nu}_{\beta\beta})^* = (M_\nu)_{ee} = (M^{\mathrm{tree}}_\nu)_{ee} + (M^{\text{1-l}}_\nu)_{ee} + \cdots \,. \tag{78}$$

For $\mathsf{CP}^{\mu\tau}$ symmetric theories, it is confined to bands depending on the CP parities of the light neutrinos [8]. For a review on generic aspects of $0\nu2\beta$ see Ref. [34]. We are assuming we are confined to the parameter space where the one-loop contributions are negligible compared to the tree-level one.

Considering (76), we can define, in analogy to the light neutrino contribution [20],

$$m^{S}_{\beta\beta} \equiv |\langle p^2 \rangle| \sum_{i=1}^{3} \frac{(\theta V_S)^2_{ei} M_{S_i}}{M^2_{S_i} + |\langle p^2 \rangle|} \,. \tag{79}$$

where $|\langle p^2 \rangle| \approx (253\,\mathrm{MeV})^2$ (corresponding to $0.079 \times (0.9\,\mathrm{GeV})^2$ in Ref. [25]) and we have already specialized to ^{76}Ge. We disregard the subdominant contribution from the heavier states N_i. If the heavy neutrinos masses are much larger than the typical momentum transfer in the nucleus, $M_i \gg 200$ MeV, we can approximate

$$m^{S}_{\beta\beta} = |\langle p^2 \rangle| \sum_{i=1}^{3} \frac{(\theta V)^2_{ei}}{M_{S_i}} \,. \tag{80}$$

Taking the GERDA+Helderberg-Moscow limit, $T^{0\nu}_{1/2}(^{76}\mathrm{Ge}) \geq 3 \times 10^{25}\mathrm{yr}$ at 90% C.L. [35], it translates into

$$\left| m^{\nu}_{\beta\beta} + m^{S}_{\beta\beta} \right| \lesssim 0.3\,\mathrm{eV} \,. \tag{81}$$

We can see that the contribution from light neutrinos predicted in our model (28) is at least two orders of magnitude smaller than the limit above. It remains to be checked if the contribution from S_i exchange can give a larger contribution.

In the limit where $\mathrm{U}(1)_{\mu-\tau}$ (or LFT) in (47) is conserved, only S_1 couples to the e flavor and thus to $0\nu2\beta$; cf. (54). We can then write

$$m_{\beta\beta}^{S_1} = -2.67\times10^{-5}\,\mathrm{eV}\times\left(\frac{m_{D_{11}}}{10\,\mathrm{keV}}\right)^2\frac{10^2}{R_{N_1}}\left(\frac{\mathrm{GeV}}{M_{S_1}}\right)^3\,, \tag{82}$$

where we have assumed that $M_{S_1}\gg 200\,\mathrm{MeV}$. For the values (70), this contribution is negligible. One could lower the M_{S_1} mass to increase this contribution (including the correction in (79)) but it hits the BBN constraint rather quickly. Such a feature is illustrated in Fig. 7 where the ratio of the $0\nu2\beta$ contribution from S_1 exchange to the limit of 0.3 eV is shown in dashed green. Note that we use the expression (79) to account for $M_{S_1}<100\,\mathrm{MeV}$. We can see that the $m_{\beta\beta}^S$ is negligible for M_{S_1} larger than 1.33 GeV. Even if we allow the life-time of S_1 to be around 1 s, it will be still unobservable in future $0\nu2\beta$ experiments. It is possible, however, that $m_{\beta\beta}^S\sim 30\,\mathrm{meV}$ for $M_{S_1}\sim 300\,\mathrm{MeV}$ and much larger than the light neutrino contribution.

VIII. CONCLUSIONS

We have presented a new CP symmetry applicable to models with A_4 flavor symmetry and other groups with the structure $H\rtimes\mathbb{Z}_3$ such as $\Delta(27)$. To implement this type of CP symmetry, the singlets $\mathbf{1}'$ that are fermions or carry other quantum numbers should appear *in pair* with another $\mathbf{1}''$ with the remaining quantum numbers identical to those of $\mathbf{1}'$. This new CP symmetry allows us to avoid the vev alignment problem in close analogy to the construction using $\mathsf{L}_\mu-\mathsf{L}_\tau$ and $\mathsf{CP}^{\mu\tau}$ symmetries [8]. This feature partly follows because the SM lepton fields are singlets of A_4 and only feel the $\mathbb{Z}_3$ subgroup which is contained in $\mathsf{L}_\mu-\mathsf{L}_\tau$.

We have constructed an explicit renormalizable model that leads to a new form for the light neutrino mass matrix, cf. (1). It retains the successful predictions of $\mathsf{CP}^{\mu\tau}$ – namely maximal θ_{23}, maximal Dirac CP phase and trivial Majorana phases – but because of the A_4 structure it also predicts normal hierarchy with the lightest neutrino of only few meV; see (27). The CP parities are also restricted to two possibilities which effectively fix the effective parameter $m_{\beta\beta}$ contributing to neutrinoless double beta decay.

The model itself is based on the extended seesaw mechanism which naturally leads to relatively light right-handed neutrinos S_i and heavier N_i. After enforcing negligible one-loop contributions to light neutrino masses, ensure the ESS approximation and require fast enough decay rate of the BSM states to avoid BBN constraints we only find a small allowed region in the parameter space: N_i neutrinos lie at the electroweak scale and the lighter S_i lie at the GeV scale. To suppress the one-

loop contributions, it is required that their Yukawa interactions with the SM fields should be smaller than the electron Yukawa coupling. Consequently the active-sterile mixing is largely suppressed, rendering the right-handed neutrinos practically unobservable in terrestrial experiments.

The flavor structure of the model is largely determined by the approximate conservation of the combination $\mathtt{L}_\mu - \mathtt{L}_\tau$ of lepton flavors, which suppresses various flavor changing processes such as $\mu \to e\gamma$. Moreover, only S_1 mixes appreciably to ν_e and the mixing of $S_{2,3}$ to the $\mu\tau$ flavors are of the same order of magnitude.

Acknowledgments

The author would like to thank the Maryland Center for Fundamental Physics of the University of Maryland at College Park, USA, for the hospitality where this work initiated. The author also thanks Rabindra Mohapatra for discussion on several points.

Appendix A: Block diagonalization of M_R

The ESS mechanism naturally leads to two disparate scales for the right-handed neutrinos: the lighter M_S (S_{iR}) and the heavier M_N (N_{iR}). So it is useful to write the complete neutrino mass matrix (35) in a basis where M_R is block diagonal:

$$\mathbb{M}' = \begin{pmatrix} 0 & M_D'^{\mathsf{T}} \\ M_D' & M_R' \end{pmatrix} \approx \begin{pmatrix} 0 & -m_D M_N^{-1}\Lambda^{\mathsf{T}} & m_D^{\mathsf{T}} \\ (-m_D M_N^{-1}\Lambda^{\mathsf{T}})^{\mathsf{T}} & M_S & 0 \\ m_D & 0 & M_N' \end{pmatrix} . \tag{A1}$$

The mass matrix M_S is given by (39). The subleading correction to M_N is

$$M_N' = M_N + \tfrac{1}{2}(\Lambda^{\mathsf{T}}\Lambda^* M_N^{*-1} + \text{tr.}) , \tag{A2}$$

where tr. indicates the transpose of the previous matrix.

The block diagonalization is performed by

$$U_R \approx \begin{pmatrix} 0 & \mathbb{1} \\ \mathbb{1} & 0 \end{pmatrix} \begin{pmatrix} \mathbb{1} - \theta_R\theta_R^\dagger/2 & \theta_R \\ -\theta_R^\dagger & \mathbb{1} - \theta_R^\dagger\theta_R/2 \end{pmatrix} , \tag{A3}$$

with

$$\theta_R^* = \Lambda\, M_N^{-1} . \tag{A4}$$

Further block diagonalization leads to the results in (39) and (40). The complete diagonalization is performed by

$$\begin{aligned}
\nu_i &\to (U_\nu)_{ij}\nu_{jL} + (\theta_{\nu S}V_S)_{ij}S^c_{jR} + (\theta_{\nu N}V_N)_{ij}N^c_{jR}\,,\\
S^c_{iR} &\to (V_S)_{ij}S^c_{jR} + (-\theta^\dagger_{\nu S}U_\nu)_{ij}\nu_{iL} + (\theta_R V_N)_{ij}N^c_{jR}\,,\\
N^c_{iR} &\to (V_N)_{ij}N^c_{jR} + (m_D^{\mathsf{T}-1}M_\nu U_\nu)_{ij}\nu_{iL} + (-\theta^\dagger_R V_S)_{ij}S^c_{jR}\,.
\end{aligned} \tag{A5}$$

The fields in the left-hand side are in the flavor basis and appear in (32); the ones on the right-hand side are the mass eigenfields and U_ν is the PMNS matrix in the flavor basis. We have neglected non-unitary effects and the small mixing angles $\theta_{\nu S}, \theta_{\nu N}, \theta_R$ were already given in Eqs. (40) and (A4).

Appendix B: Comments on the potential

Here we justify the approximate conservation of $\mathrm{U}(1)_{\mu-\tau}$ that follows from the $\mathbb{Z}_3$ conserving vevs for η in (46).

We start by observing that when the potential for η is invariant by global rephasing, the potential is identical to a potential with three Higgs doublets with A_4 symmetry and we know that (46) can be exactly a global minimum [36].

The addition of the two independent quartic terms that breaks $U(1)$ but conserves $\mathbb{Z}_4^D$,

$$I_1 = \eta_1^4 + \eta_2^4 + \eta_2^4 \quad \text{and} \quad I_2 = (\eta_1\eta_2)^2 + (\eta_2\eta_3)^2 + (\eta_3\eta_1)^2\,, \tag{B1}$$

can be chosen to maintain such alignment and also to make u_0 real and positive. We stress that these and other quartic terms are not invariant by $\mathrm{U}(1)_{\mu-\tau}$ but only the $\mathbb{Z}_3$ subgroup. These terms also help to maintain the deviations of $\langle\eta\rangle$ in the real direction since the coefficients are real because of $\mathsf{CP}^{\mu\tau}$.

Now we add the interactions of η with φ_0 and φ_1. The relevant terms are

$$V \supset \tfrac{1}{2}M_0^2\varphi_0^2 + \mu_{0\eta}\varphi_0(\eta^{\mathsf{T}}\eta + h.c.)\,, \tag{B2}$$

and

$$V \supset M_1^2|\varphi_1|^2 + \left\{\mu_{1\eta}[(\eta\eta)_{1''} + (\eta\eta)^*_{1'}]\,\varphi_1 + h.c.\right\}, \tag{B3}$$

where $\mu_{1\eta}$ can be complex and the singlet combination was defined in (33). Clearly there is no $U(1)$ rephasing symmetry for φ_1 and no Goldstone will be generated.

The mild hierarchy of ESS scales

$$100\,\text{MeV} \sim \mu_i \ll f_i'\sqrt{3}u_0 \sim 10\,\text{GeV}\,, \tag{B4}$$

implies a mild hierarchy between $u_0 \sim \langle\eta_i\rangle$ and $\langle\varphi_0\rangle, \langle\varphi_1\rangle$. We can choose $f_i' \sim 0.1$ so that $u_0 \sim 100\,\text{GeV} \sim M_N$. For an order one k_0, the small $\langle\varphi_0\rangle \sim 100\,\text{MeV}$ can be generated from (B2) by a vev seesaw analogous to type-II seesaw [37]. In this case $M_{\varphi_0} \sim u_0$ is electroweak scale. For $\langle\varphi_1\rangle$ a vev seesaw can not be implemented because $(\eta\eta)_{1''}$ vanishes for the minimum (46). But we can always take $k_1 \sim 10^{-2}$, adjust the potential parameters to obtain $\langle\varphi_1\rangle \sim 10\,\text{GeV}$ and make $\mu_{1\eta}$ in (B3) small enough so that (46) is only slightly disturbed. The mass of the lightest physical states of φ_1 will be around $\langle\varphi_1\rangle$ and heavier than S_i. Note that $k_0\langle\phi_0\rangle$ and $k_1\langle\phi_1\rangle$ should be comparable because they lead to μ_i.

At last, in principle the new scalars could be produced in Higgs decays through the Higgs portal but the current limits on the invisible Higgs decays are still weak [38] and can be avoided by decreasing the portal interactions.

Appendix C: Decay rates for S_i

In our theory the RHN heavy states S_i are the lightest new states beyond the SM which lies at the GeV scale. The dominant decay channels involve Z or W exchange through mixing with light neutrinos or charged leptons [30]. The decays $S_i^c \to S_j^c + \cdots$ are highly suppressed.

To ensure that the production of light nuclear elements in the early Universe (Big Bang nucleosinthesis) are not disturbed by the presence of new particles, we require that the life-times of the new states are shorter than 0.1 second. In that case these new particles are thermalized much before the BBN era and they decay fast enough. RHNs lighter than around 100 MeV conflict with direct detection constraints and are excluded [27, 39].

Assuming the $\text{U}(1)_{\mu-\tau}$ symmetry, the active-sterile mixing (53) leads to the dominant decay channels [30]

$$\begin{aligned} S_1^c &\to \pi^0\nu_e,\, \nu_e\bar{\nu}\nu,\, \pi^+e^-, \\ S_{2,3}^c &\to \pi^0\nu_{\mu,\tau},\, \nu_{\mu,\tau}\bar{\nu}\nu,\, \pi^+\mu^-\,. \end{aligned} \tag{C1}$$

We neglect the decay to other channels. The decay rates for these processes can be taken from

Ref. [30]:

$$
\begin{aligned}
\Gamma(S_1^c \to \pi^0 \nu_e) &= |(\theta V_S)_{e1}|^2 \frac{G_F^2 f_\pi^2 M^3}{32\pi} \left(1 - \frac{m_{\pi^0}^2}{M^2}\right)^2 , \\
\Gamma(S_2^c \to \pi^0 \nu_{\mu+\tau}) &= \left(|(\theta V_S)_{\mu 2}|^2 + |(\theta V_S)_{\tau 2}|^2\right) \frac{G_F^2 f_\pi^2 M^3}{32\pi} \left(1 - \frac{m_{\pi^0}^2}{M^2}\right)^2 , \\
\Gamma(S_1^c \to \nu_e \bar{\nu} \nu) &= |(\theta V_S)_{e1}|^2 \frac{G_F^2 M^5}{192\pi^3} , \\
\Gamma(S_2^c \to \nu_{\mu+\tau} \bar{\nu} \nu) &= \left(|(\theta V_S)_{\mu 2}|^2 + |(\theta V_S)_{\tau 2}|^2\right) \frac{G_F^2 M^5}{192\pi^3} , \\
\Gamma(S_1^c \to \pi^+ e^-) &= |(\theta V_S)_{e1}|^2 \frac{G_F^2 f_\pi^2 |V_{ud}|^2 M^3}{16\pi} \left(\left(1 - \frac{m_e^2}{M^2}\right)^2 - \frac{m_{\pi^+}^2}{M^2}\left(1 + \frac{m_e^2}{M^2}\right)\right) \\
&\quad \times \sqrt{\left(1 - \frac{(m_{\pi^+} - m_e)^2}{M^2}\right)\left(1 - \frac{(m_{\pi^+} + m_e)^2}{M^2}\right)} , \\
\Gamma(S_2^c \to \pi^+ \mu^-) &= |(\theta V_S)_{\mu 2}|^2 \frac{G_F^2 f_\pi^2 |V_{ud}|^2 M^3}{16\pi} \left(\left(1 - \frac{m_\mu^2}{M^2}\right)^2 - \frac{m_{\pi^+}^2}{M^2}\left(1 + \frac{m_\mu^2}{M^2}\right)\right) \\
&\quad \times \sqrt{\left(1 - \frac{(m_{\pi^+} - m_\mu)^2}{M^2}\right)\left(1 - \frac{(m_{\pi^+} + m_\mu)^2}{M^2}\right)} .
\end{aligned}
\tag{C2}
$$

In each expression, M refers to the mass of the decaying particle and each decay rate contributes twice due to the charge conjugate mode. Moreover, the expression for S_3^c are identical to the expressions for S_2^c and note that we can write

$$
\begin{aligned}
|(\theta V_S)_{e1}|^2 &= \frac{m_{D_{11}}^2}{M_{S_1} M_{N_1}} , \\
|(\theta V_S)_{\mu 2}|^2 + |(\theta V_S)_{\tau 2}|^2 &= \frac{m_{D_{22}}^2}{M_{S_2} M_{N_2}} \\
&= 2|(\theta V_S)_{\mu 2}|^2 = 2|(\theta V_S)_{\tau 2}|^2 .
\end{aligned}
\tag{C3}
$$

We are also assuming that $\mathrm{U}(1)_{\mu-\tau}$ is slightly broken so that $S_{2,3}$ are distinct Majorana fermions. In the exact $\mathrm{U}(1)_{\mu-\tau}$ limit, $(S_2^c + iS_3^c + S_2 + iS_3)/\sqrt{2} = S_{\mu\bar{\tau}}$ forms a Dirac heavy neutrino with $\mathrm{U}(1)_{\mu-\tau}$ charge unity while its conjugate carries charge -1. In this case, the decay rates of $S_{\mu\bar{\tau}}$ are the same as S_2^c without the factor two multiplication (the last one would be doubled due to diagonal mixing).

Appendix D: Deviations of $\mathrm{U}(1)_{\mu-\tau}$

In the fermion sector our model is approximately invariant by $\mathrm{U}(1)_{\mu-\tau}$, which includes $\mathbb{Z}_3$ (45) of A_4. In the first approximation considered $\mathrm{U}(1)_{\mu-\tau}$ is only broken in the neutrino sector by small

$\mu_i \sim 100\,\text{MeV}$ in (35). Identical $\text{U}(1)_{\mu-\tau}$ charges (47) can be assigned to all the lepton fields (47) if we change basis to

$$S^c_{iR} = (U_\omega)_{ij} S'^c_{jR}. \tag{D1}$$

We show below the form of the mass matrices in this basis with small $\text{U}(1)_{\mu-\tau}$ breaking.

An additional $\text{U}(1)_{\mu-\tau}$ (and also LFT) breaking effect in the neutrino sector is induced by deviations in $\langle\eta\rangle$ from (46), which can be parametrized as

$$\langle\eta\rangle = u_0\Big\{(1,1,1) + \epsilon_2(1,\omega^2,\omega) + \epsilon_3(1,\omega,\omega^2)\Big\}\,. \tag{D2}$$

The deviation is quantified by $|\epsilon_i| \ll 1$. $\mathsf{CP}^{\mu\tau}$ is expected to be conserved as there is no CP violating interactions for η. Hence we expect $\epsilon_3 = \epsilon_2^*$.

The mass matrices (36) in the S'_i basis read

$$\begin{aligned}
\Lambda' &= \sqrt{3}u_0 \begin{pmatrix} 1 & \epsilon_3 & \epsilon_2 \\ \epsilon_2 & 1 & \epsilon_3 \\ \epsilon_3 & \epsilon_2 & 1 \end{pmatrix} \text{diag}(f'_i)\,, \\
\mu' &= \tfrac{1}{3} \begin{pmatrix} \mu_1+\mu_2+\mu_3 & \mu_1+\omega\mu_2+\omega^2\mu_3 & \mu_1+\omega^2\mu_2+\omega\mu_3 \\ \star & \mu_1+\omega^2\mu_2+\omega\mu_3 & \mu_1+\mu_2+\mu_3 \\ \star & \star & \mu_1+\omega\mu_2+\omega^2\mu_3 \end{pmatrix}
\end{aligned} \tag{D3}$$

where the $\text{U}(1)_{\mu-\tau}$ breaking parametrization (D2) for $\langle\eta\rangle$ was used. The explicit change of basis is induced by

$$\Lambda' = U_\omega \Lambda, \quad \mu' = U_\omega \mu U_\omega\,. \tag{D4}$$

Conservation of $\mathsf{CP}^{\mu\tau}$ implies $\epsilon_3 = \epsilon_2^*$ and real μ_i. In the mass matrices it implies the usual $\mathsf{CP}^{\mu\tau}$ invariance:

$$X^{\mathsf{T}}\Lambda' X = \Lambda'^*\,, \quad X^{\mathsf{T}}\mu' X = \mu'^*\,. \tag{D5}$$

In the same basis, the S_i neutrino mass matrix (48) becomes

$$-M'^{(0)}_S = \begin{pmatrix} M^{(0)}_{S_1} & & \\ & & M^{(0)}_{S_2} \\ & M^{(0)}_{S_2} & \end{pmatrix}\,, \tag{D6}$$

where $M_{S_i}^{(0)}$ were given in (49) and we have added the superscript $^{(0)}$ to indicate the $\mathrm{U}(1)_{\mu-\tau}$ limit explicitly. A generic deviation respecting $\mathsf{CP}^{\mu\tau}$ arising from $\langle\eta\rangle$ can be parametrized by

$$-\delta M'_S = M_{S_1}^{(0)} \begin{pmatrix} 0 & z_{12} & z_{13} \\ \star & z_{22} & 0 \\ \star & \star & z_{33} \end{pmatrix} , \tag{D7}$$

where $z_{13} = z_{12}^*$, $z_{33} = z_{22}^*$.

The combination $M'_S = M_S^{\prime(0)} + \delta M'_S$ is now diagonalized by

$$V'_S = iU_{23}\mathcal{O}_\epsilon \, , \tag{D8}$$

where U_{23} denotes the maximal mixing matrix in (17). One can check that $\mathcal{O}_\epsilon$ is a real orthogonal matrix given by

$$\mathcal{O}_\epsilon \approx \begin{pmatrix} 1 & -d'_1 & -d'_2 \\ d_1 & c_\theta & -s_\theta \\ d_2 & s_\theta & c_\theta \end{pmatrix} . \tag{D9}$$

The small parameters d_i are combinations of the small quantities in (D7) and are defined by

$$-U_{23}^{\mathsf{T}}\delta M'_S U_{23} = M_{S_1}^{(0)} \begin{pmatrix} 0 & d_1 & d_2 \\ d_1 & c_1 & c_2 \\ d_2 & c_2 & -c_1 \end{pmatrix} ; \tag{D10}$$

all d_i, c_i are real. The primed d'_i are rotated as

$$\begin{pmatrix} d'_1 \\ d'_2 \end{pmatrix} = \begin{pmatrix} c_\theta & s_\theta \\ -s_\theta & c_\theta \end{pmatrix} \begin{pmatrix} d_1 \\ d_2 \end{pmatrix} , \tag{D11}$$

with angle $\tan 2\theta = c_2/c_1$. One can note that the angle θ depends only on the deviation parameters c_i and does not need to be small due to the degeneracy $M_{S_2}^{(0)} = M_{S_3}^{(0)}$. The formula (D9) is valid as long as $d_i, c_i \ll 1$ and covers the case where $M_{S_1}^{(0)} \gg M_{S_2}^{(0)} \sim M_{S_1}^{(0)} d_i \sim M_{S_1}^{(0)} c_i$ so that the mass splitting for $S_{2,3}$ can be substantial:

$$\begin{aligned} M_{S_2} &= M_{S_2}^{(0)} + M_{S_1}^{(0)}\sqrt{c_1^2 + c_2^2} \, , \\ M_{S_3} &= M_{S_2}^{(0)} - M_{S_1}^{(0)}\sqrt{c_1^2 + c_2^2} \, . \end{aligned} \tag{D12}$$

We are adopting $M_{S_3} < M_{S_2}$.

Putting all together we find the deviation from (53):

$$
\begin{aligned}
(\theta V_S) &\approx |(\theta V_S^{(0)})_{e1}|\,\mathrm{diag}(1,k,k)\begin{pmatrix} 1 & -\epsilon_3^* & -\epsilon_2^* \\ -\epsilon_2^* & 1 & -\epsilon_3^* \\ -\epsilon_3^* & -\epsilon_2^* & 1 \end{pmatrix} \times iU_{23}\mathcal{O}_\epsilon\,, \\
&= (\theta V_S^{(0)})_{e1}\,\mathrm{diag}(1,k,k) \times \begin{pmatrix} 1 & \epsilon_{12} & \epsilon_{13} \\ \epsilon_{21} & x_{22} & x_{23} \\ \epsilon_{31} & x_{32} & x_{33} \end{pmatrix}\,,
\end{aligned}
\tag{D13}
$$

where ϵ_{ij} are small parameters that depend on the small parameters $\epsilon_{2,3}$ while x_{ij} are order one, approximately unitary, quantities. The deviation from maximal (23) mixing in (53) can be large due to $S_{2,3}$ mass degeneracy in the $\mathrm{U}(1)_{\mu-\tau}$ limit. Again the superscript (0) denotes the $\mathrm{U}(1)_{\mu-\tau}$ limit. Note that (θV_S) has the structure

$$
\begin{pmatrix} u_1 & u_2 & u_3 \\ w_1 & w_2 & w_3 \\ w_1^* & w_2^* & w_3^* \end{pmatrix}\,,
\tag{D14}
$$

characteristic of $\mathsf{CP}^{\mu\tau}$ invariance [8, 11]

Considering the deviation (D13) in $\nu - S$ mixing, we can include the effects of $M_{S_{2,3}}$ exchange in $0\nu2\beta$ as

$$
m_{\beta\beta}^S = m_{\beta\beta}^{S_1}\left\{1 + \epsilon_{12}^2\frac{M_{S_1}^{(0)}}{M_{S_2}} + \epsilon_{13}^2\frac{M_{S_1}^{(0)}}{M_{S_3}}\right\}\,,
\tag{D15}
$$

where $M_{S_{2,3}}$ are now nondegenerate and include the $\mathrm{U}(1)_{\mu-\tau}$ breaking effects. It is clear that the contribution of S_2 (S_3) exchange can be comparable to S_1 exchange only if

$$
M_{S_1}/M_{S_{2,3}} \sim O(1/\epsilon^2)\,.
\tag{D16}
$$

This can not happen in our theory.

We can also confirm that $\mathrm{U}(1)_{\mu-\tau}$ breaking is not enough to induce observable lepton flavor violating processes such as $\mu \to e\gamma$. The vanishing rate is now proportional to the $\mathrm{U}(1)_{\mu-\tau}$ breaking effects. Considering only S_i in the loop, the branching ratio yields [22]

$$
B(\mu \to e\gamma) \sim 2\times10^{-30} \times \left|\frac{\epsilon_{21}}{0.1}\right|^2 \times \left|\frac{(\theta V)_{eS_1}}{10^{-6}}\right|^4 \tilde{G}_1^2\,,
\tag{D17}
$$

where $\tilde{G}_i = G(M_{S_i}^2/M_W^2) - G(0)$ and $G(x)$ is defined in Ref. [22]. For example, $G(1^2/80^2) - G(0) \approx -10^{-4}$. Therefore, the predicted rate is much below the current MEG limit $B(\mu \to e\gamma) < 2.4\times$

10^{-12} [40] and there is no constraint even if $(\theta V)_{eS_1}$ is as large as 1%. One can also check that $S_{2,3}$ contributions lead to similar results. Future $\mu \to e$ conversion experiments in nuclei [41] can improve the limit by few orders of magnitude but our model predictions are still suppressed. Hence, LFV processes constraints are much weaker than $0\nu2\beta$ in our model.

---

[1] K. Abe et al.[T2K collaboration], Phys. Rev. Lett. 107 (2011) 041801 [arXiv:1106.2822]; P. Adamson et al. [MINOS Collaboration], Phys. Rev. Lett. 107, 181802 (2011) [arXiv:1108.0015]; Y. Abe et al. [DOUBLE-CHOOZ Collaboration], Phys. Rev. Lett. 108, 131801 (2012) [arXiv:1112.6353]; F. P. An et al. [DAYA-BAY Collaboration], Phys. Rev. Lett. 108, 171803 (2012) [arXiv:1203.1669]; J. K. Ahn et al. [RENO Collaboration], Phys. Rev. Lett. 108, 191802 (2012) [arXiv:1204.0626].

[2] A. de Gouvea *et al.* [Intensity Frontier Neutrino Working Group Collaboration], arXiv:1310.4340 [hep-ex].

[3] P. F. Harrison and W. G. Scott, Phys. Lett. B **547**, 219 (2002) [arXiv:hep-ph/0210197]; W. Grimus and L. Lavoura, Phys. Lett. B **579**, 113 (2004) [arXiv:hep-ph/0305309]; Fortsch. Phys. **61**, 535 (2013) [arXiv:1207.1678].

[4] R. N. Mohapatra and C. C. Nishi, Phys. Rev. D **86**, 073007 (2012) [arXiv:arXiv:1208.2875];

[5] F. Feruglio, C. Hagedorn and R. Ziegler, JHEP **1307**, 027 (2013) [arXiv:1211.5560];

[6] M. Holthausen, M. Lindner and M. A. Schmidt, JHEP **1304** (2013) 122 [arXiv:1211.6953];

[7] M. C. Chen, M. Fallbacher, K. T. Mahanthappa, M. Ratz and A. Trautner, Nucl. Phys. B **883** (2014) 267 [arXiv:1402.0507];

[8] R. N. Mohapatra and C. C. Nishi, JHEP **1508** (2015) 092 [arXiv:1506.06788 [hep-ph]].

[9] M. C. Gonzalez-Garcia, M. Maltoni and T. Schwetz, JHEP **1411** (2014) 052 [arXiv:1409.5439].

[10] G. L. Fogli, E. Lisi, A. Marrone, D. Montanino, A. Palazzo and A. M. Rotunno, Phys. Rev. D **86** (2012) 013012 [arXiv:1205.5254 [hep-ph]]; D. V. Forero, M. Tortola and J. W. F. Valle, Phys. Rev. D **86** (2012) 073012 [arXiv:1205.4018 [hep-ph]].

[11] H. J. He, W. Rodejohann and X. J. Xu, Phys. Lett. B **751** (2015) 586 [arXiv:1507.03541 [hep-ph]]; A. S. Joshipura and K. M. Patel, Phys. Lett. B **749** (2015) 159 [arXiv:1507.01235 [hep-ph]].

[12] G. Altarelli and F. Feruglio, Rev. Mod. Phys. **82**, 2701 (2010) [arXiv:1002.0211]; S. F. King and C. Luhn, Rept. Prog. Phys. **76**, 056201 (2013) [arXiv:1301.1340].

[13] K. S. Babu, E. Ma and J. W. F. Valle, Phys. Lett. B **552**, 207 (2003) [arXiv:hep-ph/0206292].

[14] E. Ma, arXiv:1510.02501 [hep-ph]; Phys. Rev. D **92** (2015) 5, 051301 [arXiv:1504.02086 [hep-ph]]; G. N. Li and X. G. He, Phys. Lett. B **750** (2015) 620 [arXiv:1505.01932 [hep-ph]].

[15] G. J. Ding, S. F. King and A. J. Stuart, JHEP **1312** (2013) 006 [arXiv:1307.4212 [hep-ph]].

[16] C. C. Nishi, Phys. Rev. D **88** (2013) 3, 033010 [arXiv:arXiv:1306.0877 [hep-ph]].

[17] S. K. Kang and C. S. Kim, "Extended double seesaw model for neutrino mass spectrum and low scale

leptogenesis," Phys. Lett. B **646** (2007) 248 [arXiv:hep-ph/0607072].

[18] M. Mitra, G. Senjanovic and F. Vissani, Nucl. Phys. B **856** (2012) 26 [arXiv:1108.0004 [hep-ph]].

[19] E. Ma, Phys. Rev. D **82** (2010) 037301 [arXiv:1006.3524 [hep-ph]].

[20] M. Blennow, E. Fernandez-Martinez, J. Lopez-Pavon and J. Menendez, JHEP **1007** (2010) 096 [arXiv:1005.3240 [hep-ph]]; J. Lopez-Pavon, S. Pascoli and C. f. Wong, Phys. Rev. D **87** (2013) 9, 093007 [arXiv:1209.5342 [hep-ph]].

[21] P. Hernandez, M. Kekic and J. Lopez-Pavon, Phys. Rev. D **90** (2014) 6, 065033 [arXiv:1406.2961 [hep-ph]]; Phys. Rev. D **89** (2014) 7, 073009 [arXiv:1311.2614 [hep-ph]].

[22] A. Ibarra, E. Molinaro and S. T. Petcov, Phys. Rev. D **84** (2011) 013005 [arXiv:1103.6217 [hep-ph]]; JHEP **1009** (2010) 108 [arXiv:1007.2378 [hep-ph]].

[23] W. Grimus and L. Lavoura, Phys. Lett. B **546** (2002) 86 [arXiv:hep-ph/0207229]; W. Grimus and H. Neufeld, Nucl. Phys. B **325** (1989) 18. A. Pilaftsis, Z. Phys. C **55** (1992) 275 [arXiv:hep-ph/9901206].

[24] D. Aristizabal Sierra and C. E. Yaguna, JHEP **1108** (2011) 013 [arXiv:1106.3587 [hep-ph]].

[25] J. Lopez-Pavon, E. Molinaro and S. T. Petcov, JHEP **1511** (2015) 030 [arXiv:1506.05296 [hep-ph]];

[26] P. S. B. Dev and A. Pilaftsis, Phys. Rev. D **86** (2012) 113001 [arXiv:1209.4051 [hep-ph]].

[27] O. Ruchayskiy and A. Ivashko, JCAP **1210** (2012) 014 [arXiv:1202.2841 [hep-ph]].

[28] F. F. Deppisch, P. S. Bhupal Dev and A. Pilaftsis, New J. Phys. **17** (2015) 7, 075019 [arXiv:1502.06541 [hep-ph]]; M. Drewes and B. Garbrecht, arXiv:1502.00477 [hep-ph].

[29] A. de Gouvêa and A. Kobach, arXiv:1511.00683 [hep-ph].

[30] D. Gorbunov and M. Shaposhnikov, JHEP **0710** (2007) 015 [JHEP **1311** (2013) 101] [arXiv:0705.1729 [hep-ph]]; A. D. Dolgov, S. H. Hansen, G. Raffelt and D. V. Semikoz, Nucl. Phys. B **590** (2000) 562 [arXiv:hep-ph/0008138].

[31] F. del Aguila and J. A. Aguilar-Saavedra, Nucl. Phys. B **813** (2009) 22 [arXiv:arXiv:0808.2468 [hep-ph]]; Phys. Lett. B **672** (2009) 158 [arXiv:0809.2096 [hep-ph]]; F. del Aguila, J. A. Aguilar-Saavedra and R. Pittau, JHEP **0710** (2007) 047 [arXiv:hep-ph/0703261].

[32] Q. H. Cao, A. Damanik, E. Ma and D. Wegman, Phys. Rev. D **83** (2011) 093012 [arXiv:1103.0008 [hep-ph]].

[33] A. Ilakovac and A. Pilaftsis, Nucl. Phys. B **437** (1995) 491 [arXiv:hep-ph/9403398].

[34] W. Rodejohann, Int. J. Mod. Phys. E **20** (2011) 1833 [arXiv:1106.1334 [hep-ph]]; C. Aalseth *et al.*, arXiv:hep-ph/0412300.

[35] M. Agostini *et al.* [GERDA Collaboration], Phys. Rev. Lett. **111** (2013) 12, 122503 [arXiv:1307.4720 [nucl-ex]]; J. B. Albert *et al.* [EXO-200 Collaboration], Nature **510** (2014) 229 [arXiv:1402.6956 [nucl-ex]]. Y. Huang and B. Q. Ma, The Universe **2** (2014) 65 [arXiv:1407.4357 [hep-ph]].

[36] I. P. Ivanov and C. C. Nishi, JHEP **1501** (2015) 021 [arXiv:1410.6139 [hep-ph]].

[37] J. Schechter and J. W. F. Valle, Phys. Rev. D **22** (1980) 2227; M. Magg and C. Wetterich, Phys. Lett. B **94** (1980) 61; T. P. Cheng and L. F. Li, Electroweak Phys. Rev. D **22** (1980) 2860. G. Lazarides, Q. Shafi and C. Wetterich, Nucl. Phys. B **181** (1981) 287; R. N. Mohapatra and G. Senjanovic, Phys.

Rev. D **23** (1981) 165;

[38] The ATLAS collaboration [ATLAS Collaboration], "Search for an Invisibly Decaying Higgs Boson Produced via Vector Boson Fusion in pp Collisions at $\sqrt{s} = 8$ TeV using the ATLAS Detector at the LHC," ATLAS-CONF-2015-004.

[39] A. D. Dolgov, S. H. Hansen, G. Raffelt and D. V. Semikoz, Nucl. Phys. B **590** (2000) 562 [arXiv:hep-ph/0008138]; Nucl. Phys. B **580** (2000) 331 [arXiv:hep-ph/0002223]; A. Kusenko, S. Pascoli and D. Semikoz, JHEP **0511** (2005) 028 [arXiv:hep-ph/0405198].

[40] J. Adam *et al.* [MEG Collaboration], Phys. Rev. Lett. **107** (2011) 171801, [arXiv:1107.5547 [hep-ex]].

[41] R. Alonso, M. Dhen, M. B. Gavela and T. Hambye, "Muon conversion to electron in nuclei in type-I seesaw models," JHEP **1301** (2013) 118 [arXiv:1209.2679 [hep-ph]].